Acta Crystallographica Section B
Structural Science
ISSN 0108-7681

Architecture of crystal structures from square planes

J. Hauck* and K. Mika

Institut für Festkörperforschung, Forschungszentrum Jülich, D-52425 Jülich, Germany

Correspondence e-mail: j.hauck@fz-juelich.de

Received 1 May 1998
Accepted 27 April 2000

The crystal structures of ordered b.c.c. (body-centered cubic), f.c.c. (face-centered cubic) or primitive cubic alloys A_xB_y and related NaCl, ZnS or CaF_2 derivative structures are characterized by the self-coordination numbers T_1, T_2 of the A atoms with A atoms. Structures with identical T_1 and T_2 values for all A atoms are at the corners of T_1 and T_2 structure maps, and can be analyzed for attractive or repulsive interactions of A atoms. Most observed structures are at the borders of the structure map and can be obtained by ~10 different combinations of structural units. The different combination mechanisms explain *e.g.* the shear structures of CuAu II or Nb_2O_5 and the occurrence of vacancies in NaCl-related structures like NbO.

1. Introduction

A large number of crystal structures can be described as ordered body-centered cubic (b.c.c.), face-centered cubic (f.c.c.) or primitive cubic (p.c.) compounds A_xB_y or as NaCl, ZnS or CaF_2 derivative structures (Villars & Calvert, 1986; Parthé *et al.*, 1993) with a distribution of A and B atoms on different positions. The number of observed structures is small compared with the number of all possible structures, which is 2^{n-1} for a unit cell with n possible positions of A or B atoms. All reduced unit cells of the b.c.c., f.c.c. and p.c. lattice with $n \leq 9$ atom positions were determined and the different structures selected numerically in the present investigation. The theoretical structures can be sorted for different aspects such as high symmetry, single coordination numbers or the extent to which Pauling's rules (Pauling, 1929) are obeyed. Pauling's rule of parsimony is particularly useful for the selection: 'The number of essentially different kinds of constituents in a crystal tends to be small'. The polyhedra circumscribed about all chemically identical atoms should, if possible, be chemically similar and similar in the nature of the sharing of corners, edges and faces with other polyhedra. This explanation is similar to the Wiener–Sohncke principle: 'Points are disposed around each point in the same way as around every other' (Wiener, 1863; Sohncke, 1879; Brunner, 1971). We have selected the self-coordination numbers (s-CN) of A atoms with A atoms as parameters to characterize these structures (§2). Table 1 shows the maximum s-CN values $T_i^{\max}$ for coordination shells i = 1–10 for a variety of structures, which can be obtained from the square lattice. The maximum values are reduced if some of these positions are occupied by B atoms in A_xB_y (Fig. 1). A large number of possible structures can be characterized by these T_i values and homometric structures (structures with identical T_i values, §3) can be

differentiated by different space groups. The T_i values can be plotted in T_1, T_2 structure maps such as those shown in Fig. 2.

The large variety of orderings of atoms in A_xB_y is characterized by the number of nearest, next-nearest and third-nearest neighbors of A atoms, T_1, T_2 and T_3, and the ratio of A and B atoms $y/x \geq 1$. The T_1 T_2 T_3; y/x values of the minority component A are sufficient to characterize an undistorted structure. The self-coordination numbers T_1, T_2 and T_3 of the A atoms with A atoms in A_xB_y compounds can be plotted to create a T_1, T_2 or T_1, T_2, T_3 structure map such as that shown in Fig. 2.

The numerical procedure to obtain a structure map will be outlined for a single square layer occupied by A and B atoms (Fig. 1*a*). The procedure contains the following steps:

(i) The unit cell of the square layer is increased by adding more squares and the corners of the squares occupied by A and B atoms (Fig. 1*b*).

(ii) The positions at the corners are occupied with A atoms to a maximum of 50% at $y/x \geq 1$. The structures at higher A content are identical by exchange of the A and B atoms.

(iii) The different crystal structures are characterized by the coordination of the A atoms with other A atoms in the first, second and third coordination shells T_1, T_2 and T_3, and the ratio y/x of B to A atoms, *e.g.* the notation 2 0 4; 1 is used for the structure with $T_1 = 2A$ atoms at distance a, no A atoms in the second coordination shell at distance $2^{1/2}a$, $T_3 = 4A$ atoms at distance $2a$ and $y/x = 1$. $T_1^{\max} = T_2^{\max} = T_3^{\max} = 4$ are the maximum self-coordination numbers of the square layer. The coordination numbers of each shell are averaged for structures which have differently coordinated A atoms, *e.g.* the 0 4 2, 2 0 2 and 1 2 4 (twice) coordination numbers of the four A atoms are averaged in the 1 2 3; 1 structure.

(iv) The crystal structures characterized by the coordination numbers T_1, T_2 and T_3, and a fixed composition y/x can be plotted as single points in a three-dimensional T_1, T_2, T_3 graph (§3) or as a projection in the T_1, T_2 plane as shown in Figs. 1*b* and 2. All structures with $y/x = 1$ are found to fall within a triangle, with the three structures 4 4 4; (1), 2 0 4; 1 and 0 4 4; 1 at the corners. The structure 4 4 4; (1) with the composition given by (1) in brackets can only be obtained in the limit of very large unit cells, because the boundary line between the A and B clusters prevents an exact realisation 4 4 4; 1 for finite cells. The 4 4 4; (1) values are also valid for an occupation of all sites by A atoms.

(v) The structures with $y/x = 1$ shown on the structure map can be considered as combinations of the variously shaded squares containing different numbers of A atoms and different configurations (*cis* and *trans*) for the occupation of two positions (Fig. 1*b*). The 0 4 4; 1 and 2 0 4; 1 structures at the right-hand and upper corners of the triangle (Figs. 1 and 2) consist of squares containing two A atoms in opposite *trans* or neighboring *cis* configurations, respectively. The other structures at the right-hand side with the same composition as *e.g.* 1 2 3; 1 can be obtained by a combination of the two structural units of 0 4 4; 1 and 2 0 4; 1 (shown with different shading). The 4 4 4; (1) structure at the left-hand corner of the triangle can be considered as complete segregation of A and B atoms with complete occupancy of the squares by A or B atoms, respectively. These structural units can be combined with squares containing two A atoms in a *cis* configuration to the structures at the left-hand border of the triangle. Points within the triangle are obtained by the combination of all structural units.

Table 1
Maximum self-coordination numbers (s-CN values) $T_i^{\max}$ and radii R_i of shells in units of $a_0/2$ (CaF_2, perovskite series, face-centered cubic, body-centered cubic lattice) or a_0 (square net) for the first to the tenth coordination of A atoms with A atoms (A_xB_y), F with F atoms (CaF_2) or O atoms with O atoms (perovskite series), respectively.

	p.c./CaF_2		Perovskite		f.c.c.		b.c.c.		Square	
i	T_i	R_i^2	T_i	R_i^2	T_i	R_i^2	T_i	R_i^2	T_i	R_i^2
1	6	1	4	1	12	2	8	3	4	1
2	12	2	8	2	6	4	6	4	4	2
3	8	3	8	3	24	6	12	8	4	4
4	6	4	6	4	12	8	24	11	8	5
5	24	5	16	5	24	10	8	12	4	8
6	24	6	16	6	8	12	6	16	4	9
7	12	8	12	8	48	14	24	19	8	10
8	30	9	20	9	6	16	24	20	8	13
9	24	10	16	10	36	18	24	24	4	16
10	24	11	24	11	24	20	32	27	8	17

(vi) The s-CN values T_i^A and T_i^B of A and B atoms are different for $y/x > 1$. The s-CN values of the minority component A are plotted in Fig. 2 for A_xB_y, $y/x \geq 1$. The left-hand border of the structure map is common for all values of y/x, whereas the right-hand border is different for different y/x values, as indicated by a broken line for $y/x = 2$ in Fig. 2. An alternative way of representing the structure diagram is to use the Cowley–Warren short-range order parameter α_i (Hauck, 1980), as defined in (1) and (2) below. This can have values $-1 \leq \alpha_i \leq 1$ and can be obtained from the self-coordination numbers (s-CN) T_i^A and T_i^B of A and B atoms or from the T_i^A and y/x values (Hauck & Mika, 1994) by means of (1)–(6).

$$\alpha_i = 1 - p_i^B/y', \tag{1}$$

$$y' = y/(x + y), \tag{2}$$

$$T_i^B = T_i^{\max} - (T_i^{\max} - T_i^A)x/y, \tag{3}$$

$$\alpha_i T_i^{\max} = T_i^A + T_i^B - T_i^{\max}, \tag{4}$$

$$\alpha_i T_i^{\max} = T_i^A - (T_i^{\max} - T_i^A)x/y, \tag{5}$$

$$T_i^{\max} = T_i^A + T_i^{AB}. \tag{6}$$

p_i^B is the probability of finding a B atom in the ith coordination shell of an A atom. y' is the fraction of B atoms in A_xB_y as given by (2). The coordination numbers CN = T_i^{AB} of A atoms coordinated by B atoms are related to T_i^A by (6). Structures with compositions $y/x > 1$ can be obtained by using other structural units. The 0 0 4; 3 structure at the top-right corner of

the structure map for $y/x = 3$ (Fig. 2) contains only squares with single occupancy. The 2 0 2; 3 structure contains squares with *cis* occupation or without A atoms similar to that for $y/x = 1$. The structures on the right-hand border as *e.g.* 0 2 2; 2 can also be obtained by structural units similar to those for $y/x = 1$, however, with different concentrations of units containing zero, single or double (*trans*) occupation.

The 2 0 2; 2, 1 0 3; 2 and 0 2 2; 2 structures at the corners of the $y/x = 2$ field each consist of a combination of two structural units only. Structures at the borders as *e.g.* 3 2 2; 2 or inside the $y/x = 2$ field contain three or more structural units, respectively.

(vii) The α_i values are zero for a random distribution of A and B atoms, because the mean value of $T_i^A + T_i^B$ equals $T_i^{\max}$, which corresponds *e.g.* to $T_1 = T_2 = T_3 = 2$ at composition $y/x = 1$ (Fig. 2). Very small α_i values are expected for A_xB_y with very weak interactions between A and A or B and B atoms and in particular at high temperatures. Positive α_1 values are obtained for attractive interactions of A atoms, *i.e.* for cluster formation or segregation. The 2 0 2; 2 and 3 2 2; 2 structures of Fig. 1(*b*) consist of single and double rows of A atoms, respectively. Proceeding down the left-hand border of the structure map (Fig. 2) corresponds to increasing size of the A and B clusters until complete segregation of A and B atoms occurring in the 4 4 4; (1) structure. Negative α_1 values indicate repulsive interactions such as Coulomb repulsion between A atoms.

(viii) Two-dimensional square structures are observed *e.g.* for gas molecules adsorbed on the (100) surfaces of b.c.c. metals (MacLaren *et al.*, 1987). The extent of occupation of the surface of the metal atoms with gas molecules depends on the size of the gas molecules, the equilibrium gas pressure and the interaction between the molecules. The unit cell is usually described by the length of the two sides $l_1 \times l_2$ relative to the underlying b.c.c. cell (Hauck & Mika, 1994, 2000*b*; MacLaren *et al.*, 1987). There are different structures with identical unit cells for the occupation of two or more positions, as can be seen by the two 2×3 structures 1 0 3; 2 and 0 2 2; 2 (Fig. 1*b*).

(ix) Other structures such as *e.g.* 0 0 4; 3 and 0 4 4; 1 at the right-hand border of the structure map have the same cell size, but different concentrations. An 0 0 4; 3 structure of metal atom A can be combined with a second 0 0 4; 3 structure of A' at the center to give $AA'B_2$ or A_2B_2 with an 0 4 4; 1 structure. This type of combination of structural units is quite frequent in ordered b.c.c., f.c.c. and p.c. alloys (§§3–5).

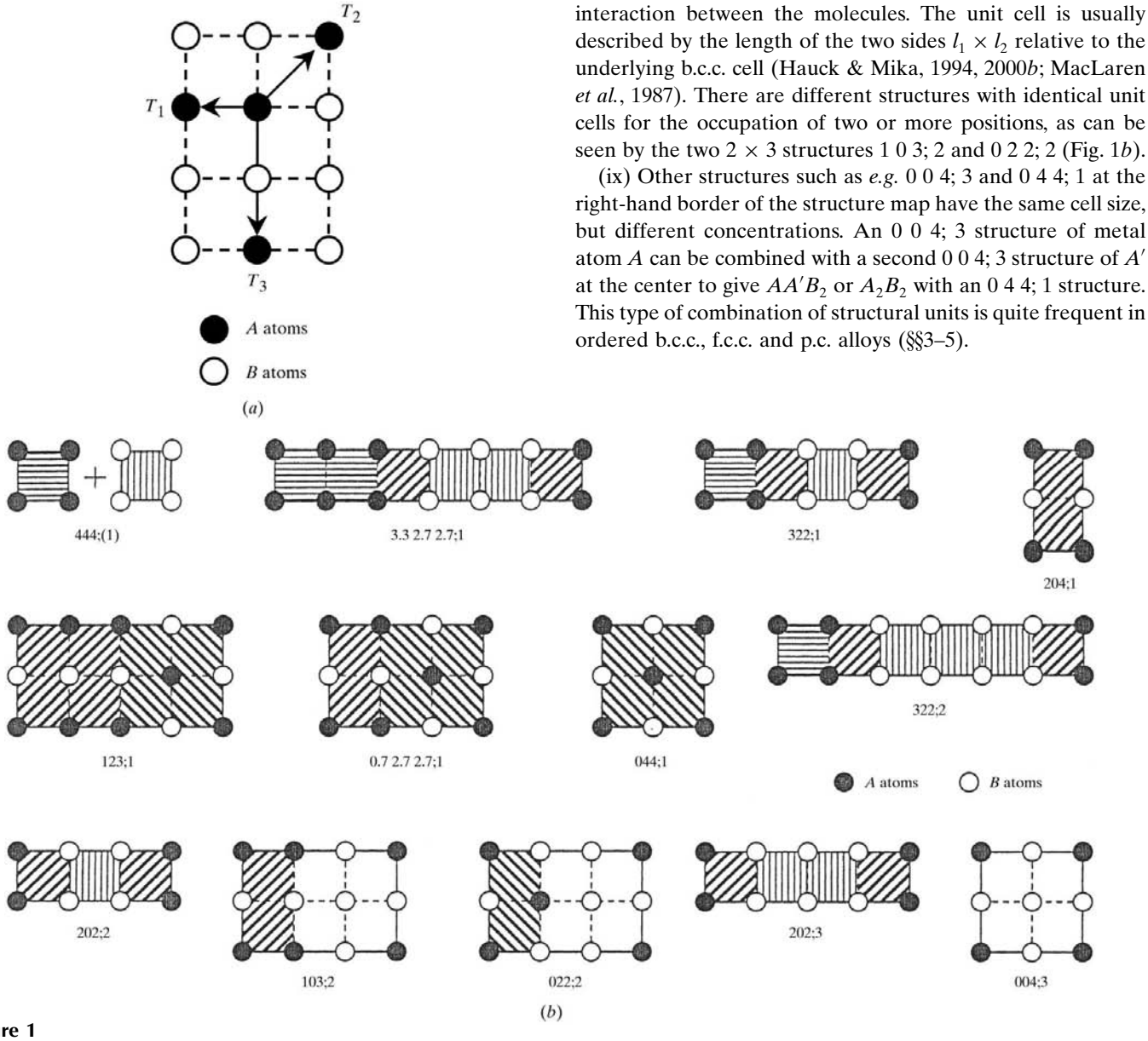

Figure 1
(*a*) Self-coordination of A atoms by nearest, next-nearest and third-nearest A atoms T_1, T_2 and T_3 in square planes. (*b*) The structures of planar A_xB_y compounds denoted as $T_1\ T_2\ T_3$; y/x contain squares with 0–4 A atoms (•) with a different shading of these structural units.

The most important structures at the corners of the structure map have a single set of T_i values such as 2 0 4; 1, 0 4 4; 1 and 0 0 4; 3 in Fig. 1(*b*). The structures at the corners and along borders of the triangular structure map (for $y/x = 1$) can be analyzed for different interactions between *A* atoms and a combination of structural units at the borders can be used to vary these interactions. The three corners of the structure map correspond to repulsive interactions between *A* atoms (*e.g.* Coulomb repulsion) in opposite *trans* positions (0 4 4; 1 structure), attractive interactions (*e.g.* covalent bonding) for *A* atoms in neighboring *cis* positions (2 0 4; 1 structure), and segregation of *A* and *B* atoms in 4 4 4; (1). Since in this case the crystal splits into all *A* and all *B* regions, the composition cannot be obtained for finite unit cells and is indicated by placing *y*/*x* in parentheses [step (iv), Fig. 1*b*]. The observed structures found in more complex systems are those on the right-hand border and in particular the structures at the corners of the structure map (2 0 4; 1, 0 4 4; 1 and 0 0 4; 3; Hauck & Mika, 1994). The coordination number of the *A* atoms by nearest neighbor *B* atoms CN = $4 - T_1$ increases from 2 in 2 0 4; 1 to 4 in 0 4 4; 1.

Pauling's rule of parsimony is obeyed for these structures: The number of essentially different kinds of constituents in a crystal tends to be small (Pauling, 1929, 1960; Burdett, 1995). Structures, in which all *A* and all *B* atoms have the same coordination sequence (T_i), *e.g.* 2 0 4; 1 and 0 4 4; 1 in Fig. 1, are usually highly symmetric, whereas structures containing *A* atoms with different environments, such as *e.g.* 1 2 3; 1 or 3 2 2; 1 in Fig. 1(*b*), are built from different structural units. The symmetry of these structures is usually lower because of the different symmetry of the structural units (Hauck & Mika, 1994). In most cases, the experimentally observed symmetry is identical with the symmetry determined for the undistorted lattice. Sometimes the symmetry is decreased because of the Jahn–Teller effect of transition metal *d* electrons or because of a lone pair of main group elements such as Bi^{3+}. The structures at the top and right-hand corners of the structure map also obey Pauling's electrovalence rule: The electrovalence of each *B* atom in A_xB_y should be compensated by the charge *q* of the *z* neighboring *A* atoms with coordination number CN ($\sum zq/\mathrm{CN}$ = charge of *B* atoms; Pauling, 1929, 1960; Burdett, 1995). The 2 0 4; 1 and 0 4 4; 1 structures of Fig. 1 for oxide layers *A*O (*i.e.* *B* = oxygen) with divalent *A* atoms contribute the total electrovalence 2 to O atoms and compensate their formal charge −2. On the other hand, one of the three different O atoms of the 1 2 3; 1 structure with electrovalencies 1.84, 2 and 2.33 does not obey Pauling's electrovalence rule within the allowed deviation of ∼1/6 (1.83 − 2.17). Most electrovalencies of f.c.c., b.c.c. or p.c. structures of the right-hand borders of the structure maps are within this limit (§6).

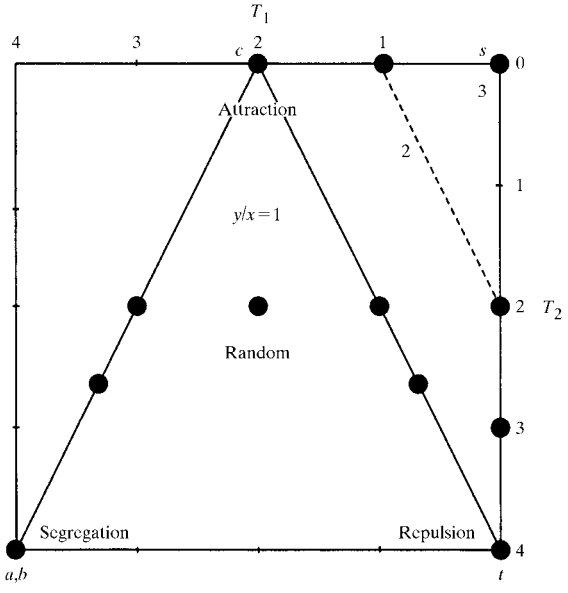

Figure 2
T_1, T_2 structure map of ordered A_xB_y crystal structures $T_1\,T_2\,T_3$; *y*/*x* of square layers. The structures of Fig. 1 (•) are at the boundaries of the structure map, which vary at the right-hand side for different *y*/*x*. The *A* atoms of the *AB* alloys ($y/x = 1$) are segregated in 4 4 4; (1), attracted in 2 0 4; 1, repelled in 0 4 4; 1, or random in 2 2 2; 1.

The square-planar layers of Fig. 1(*b*) can be packed to give the body-centered cubic (b.c.c.) or face-centered cubic (f.c.c.) lattice with the lattice constants a_1 and a_2, respectively. The *A* atoms in the center of the b.c.c. cell (• in Fig. 3) have $T_1 = 8$ nearest neighbors at the distance $a_1 3^{1/2}/2$ and $T_2 = 6$ second-nearest neighbors at the distance a_1. The self-coordination numbers (s-CN) of nearest neighbors T_1 increase from 8 in b.c.c. to 12 in the f.c.c. lattice (Table 1). Many NaCl, CaF_2 and $CaTiO_3$ related structures can also be obtained from square layers with an ordering of Cl, F or O atoms and vacancies. The Cl atoms of NaCl form an f.c.c. lattice and the F atoms of CaF_2 a primitive cubic (p.c.) lattice. In $CaTiO_3$ the two positions of the p.c. lattice (○ in Fig. 3) are occupied by metal atoms such as Ca and Ti and three positions by vacancies. In NaCl four positions are occupied by Na atoms. Fig. 3 shows the T_i values of Cl atoms in NaCl, F atoms in CaF_2 and O atoms and vacancies in the $CaTiO_3$ series.

The metal atoms such as Ca and Ti of $CaTiO_3\square_3$ and the interstitial O atoms and vacancies □ at pseudo-octahedral sites [(6*b*) positions of $Im\bar{3}m$] form together a primitive cubic structure with lattice constant $a_0/2$ similar to the F atoms of CaF_2 (Fig. 3). $CaTiO_3$ and most superconducting oxides are in this group (Hauck & Mika, 1997, 1998*b*; Hauck *et al.* 1999). The maximum s-CN values of the atoms lying on a p.c. lattice ($T_1 = 6$, $T_2 = 12$, $T_3 = 8$) are decreased for O atoms in the $CaTiO_3$ series ($T_1 = 4$, $T_2 = 8$, $T_3 = 8$), because of the metal atoms (○) at two positions of the p.c. lattice.

Previous investigations (Hauck *et al.*, 1988*a*,*b*, 1989; Hauck & Mika, 1993, 1994) have shown that the structures are most likely to be found at the borders of the structure map. All *A* (and all *B*) atoms of 8 b.c.c., 17 f.c.c. and 18 p.c. structures at the corners of the structure maps have the same set of T_i values (single sets for *A* and *B* atoms, $M^i = 2$), as was required by the Wiener–Sohncke principle. Four f.c.c. and four p.c. structures have identical T_1 and T_2 values. The remaining 20 b.c.c., 9 f.c.c. and 20 p.c. structures with the same sets of T_i values for *A* and *B* atoms are not at the boundaries of the structure map (§§3–5).

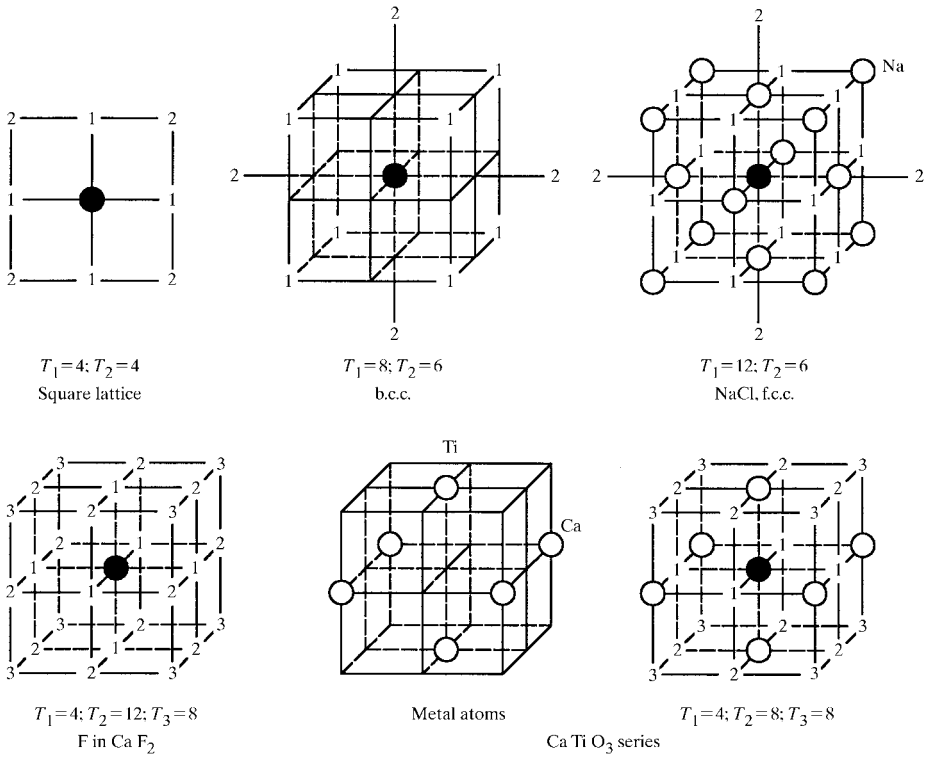

Figure 3
Coordination polyhedra for the square, body-centered metal (b.c.c.), NaCl (f.c.c. lattice of Cl atoms), primitive cubic (p.c. F atoms in CaF_2) and the O atom lattice in $CaTiO_3$ and related structures with all possible sites for O atoms [6(*b*) position of $Im\bar{3}m$; perovskite series]. The central atom is shown by a filled circle (•) and the neighbors are shown by numbers with (1) for nearest, (2) for next-nearest and (3) for third-nearest neighbor positions. Some positions of the primitive cubic lattice are occupied by other atoms shown as open circles (○), *e.g.* Na in the NaCl and Ca, Ti in the $CaTiO_3$ derivative structures. Note that in $CaTiO_3$ not all the neighboring sites are occupied by O.

Some of these structures were also obtained using different Ising methods such as Monte Carlo simulations (Ducastelle, 1991) by assuming different interaction energies V_i^{AA}, V_i^{BB} and V_i^{AB} between $A-A$, $B-B$ and $A-B$ bonds in the ith shell (§2) or by the investigation of homogeneous sphere packing (Koch & Fischer, 1992). The *ab initio* crystal structure predictions by the Ising method are limited by the rapid increase in the values of V_i, where V_i is the interaction constant of the ith shell, with increased cluster size (Sanchez & de Fontaine, 1981). The structures with the same T_i values for all A and B atoms (§2) can be compared with homogeneous sphere packings, in which the A or B atom positions are vacant. The number of contacts between homogeneously packed spheres corresponds to the T_1 values of A or B atoms. In some cases T_1 will be zero and the number of contacts corresponds to the T_2 values. A small number of different types of homogeneous sphere packing, which is important for ordered b.c.c., f.c.c. and p.c. structures, is selected in the present investigation. These structures are shown on T_1, T_2 structure maps and the relationship between different structures is outlined for different structure families. Most observed structures (§§3–5) can be described by a combination of structural units such as the structures of the Ruddlesden–Popper structure family. The T_1 and T_2 values vary linearly at the borders of the structure map and the neighborhood of A atoms changes gradually with a minimum of different surroundings, as is required by Pauling's rule of parsimony. The structures can be assembled from structural units similar to a jigsaw puzzle. Most series of structures (structure families) can be described by a linear sequence of structural units. Therefore, the total number of structures at the borders of the structure maps is to a large extent limited. Up to four structural units labeled a and b, for example, can be combined to the six sequences ab, a_2b_2, ab_2, ab_3, a_2b and a_3b (Hauck *et al.*, 1999). The combination of structural units such as squares with two A atoms in *cis* or *trans* configurations was outlined for the square-planar net (Fig. 1*b*).

The structure maps of b.c.c., f.c.c. and p.c. lattices will be analyzed in §§3–5 for ∼100 structural units. Only a few structural units in about 10 different series of structures with varying degrees of repulsive (ionic) and attractive (covalent) bonding are observed. The correlation between distorted b.c.c. and f.c.c. alloys or NaCl, ZnS and perovskite-related structures will be discussed in §6. The close relation of structures obtained from square planes can also be visualized by many identical projection patterns or identical space groups and Pearson symbols (§6). Some structures can be considered as an intergrowth of b.c.c., f.c.c. and p.c. or CaF_2 slabs (Parthé *et al.*, 1993; Kripyakevich & Grin, 1979; Pani & Fornasini, 1990). Most of the slabs in these compounds with different ordering of metal atoms are very similar to the structural units of the present investigation.

2. Ising-type analysis of structure families

We have investigated the borders of structure maps for ordered b.c.c., f.c.c. and p.c. A_xB_y structures with the following numerical procedure, similar to those outlined in previous investigations (Hauck *et al.*, 1988*b*,*c*, 1989; Mika *et al.*, 1989; Hauck & Mika, 1993, 1994):

(*a*) Determination of all reduced unit cells (Křivý & Gruber, 1976) with a maximum of nine sites for A or B atoms (Tables 1A–3A of deposited material[1]). The lattice constants $a_0 = 2$ allow integer values for the cell parameters and x, y, z coordinates of atoms.

(*b*) Occupation of sites in different concentrations and configurations.

[1] Supplementary data for this paper are available from the IUCr electronic archives (Reference: BR0078). Services for accessing these data are described at the back of the journal.

(*c*) Selection of A_xB_y structures T_1 T_2 T_3; y/x with identical s-CN values and composition y/x.

(*d*) Elimination of identical structures.

(*e*) Projection in different directions.

(*f*) Determination of the space group (Mika *et al.*, 1994).

The T_1, T_2 and T_3 values were plotted for different y/x values to create three-dimensional structure maps and the structures on the borders were analyzed for structural units (such as the squares with *A* in *cis* and *trans* configurations in Fig. 1). The structures with larger unit cells could be constructed as soon as the structural units were known.

Some structures of the present compilation were obtained by a different method (Ising model), as will be outlined briefly in the following: At high temperatures many binary alloys A_xB_y adopt a disordered form of one of the common crystal structures of metals: cubic close-packed (c.c.p.), hexagonal close-packed (h.c.p.) or body-centered cubic (b.c.c.). At lower temperatures the different metal atoms *A* and *B* order because of decreased entropy of mixing and increased attractive or repulsive interaction constants $\pm|V_i|$ in the *i*th coordination shell, $i = 1, 2, ...$, where $V_i = V_i^{AA} + V_i^{BB} - 2V_i^{AB}$ is given by the interaction energies between $A-A$, $B-B$ and $A-B$ bonds in the *i*th shell (Kanamori & Kakehashi, 1977); $V_i > 0$ favors $A-B$ bonds, $V_i < 0$ favors $A-A$ and $B-B$ bonds (Ducastelle, 1991; Allen & Cahn, 1972). These authors have derived sets of ordered structures applying the Ising model with V_1, V_2 or ratios V_2/V_4 and V_3/V_4 as parameters.

An analysis of these A_xB_y structures has shown that the *B* atoms of many structures exhibit not a single coordination as the *A* atoms do, but two to five different self-coordination numbers T_i^B for different *B* atoms in the same structure. In a few cases the different T_i^B values start to deviate with a slightly different coordination only in a higher coordination shell, *e.g.* in the sixth coordination.

3. Body-centered cubic alloys A_xB_y

We have determined numerically the structures A_xB_y with a single coordination ($M^i = 2$, §2) up to the 10th shell of all *A* and *B* atoms with an upper bound of $x + y = 9$ for b.c.c. structures. Of the 27 b.c.c. structures thus obtained (Table 2*a*, Fig. 1A, deposited), 10 b.c.c. structures were previously derived by the Ising model (Finel & Ducastelle, 1984). These 10 structures are at the corners of the T_1 T_2 T_3; y/x structure map. Only the five ordered compounds 4 4 4; 1a (γ-TiCu), 4 0 12; 1 (NaTl), 0 6 12; 1 (CsCl), 2 0 6; 2 ($CeCd_2$) and 0 4 4; 2 ($MoSi_2$) are observed. Approximately 40 other observed structures (Table 2*b*, Fig.2A, deposited) are on the borders of the T_1, T_2, T_3 structure map (Fig. 4). The six structures with $y/x = 1$ (0 6 12; 1, 2 4 6; 1, 4 0 12; 1, 4 2 4; 1, 4 4 4; 1, 6 4 6; 1), and the 8 6 12; (1) structure (corresponding to segregation of *A* and *B* atoms) are at the seven corners (*C*) of a polyhedron in the T_1, T_2, T_3 coordinate system containing 15 edges (*E*; Hauck & Mika, 1997). With Euler's formula $C + P = E + 2$, topological consistency requires $P = 10$ planes. The decahedron is projected as a triangle in the T_1, T_2 coordinate system (Fig. 4) with 0 6 12; 1 (CsCl) (repulsion), 4 0 12; 1 (NaTl) (attraction) and 8 6 12; (1) (segregation) as corners. The other structures are inside the triangle (Fig. 4). Structures such as 2 3 12; (1) or 6 3 12; (1) at the borders of the T_1, T_2 structure map (Fig. 4) can only be obtained as suprema in the limit of very large unit cells in a similar way to 8 6 12; (1). The other structures along the edges of the T_1 T_2 T_3; y/x structure map allow the analysis of architecture by structural units. Figs. 1A(*a*)–(*d*) (deposited) show most structures at the corners of the structure map projected in several different directions to illustrate the different structural units for structures on different edges of the T_1, T_2, T_3 structure map (Hauck & Mika, 1997).

There are 10 b.c.c. homometric structures, as indicated by curly brackets in Table 2(*a*) – structures with an identical coordination (all T_i) of all atoms. The homometric crystal structures cannot be distinguished by powder patterns of X-ray or neutron diffraction if the lattice is undistorted. They are labeled with *a* and *b* in Fig. 1A (deposited) and are bracketed in Tables 2–6. In other ('quasi-homometric') structures the T_i^B values of the majority component *B* deviate at higher coordination numbers as *e.g.* in 2 0 0; 7a,b or 0 2 2; 7a,b (Table 1A, deposited) or T_i^A and T_i^B values of both *A* and *B* components deviate for $i > 3$.

Some structures in Table 2(*a*) exhibit identical Cowley short-range order parameters α_i, but have different compositions y/x. These series of homologous structures have identical unit cells which are filled up successively by *A* atoms until $T_i^{\max}$ is reached (Table 3). Each *A* and each *B* atom of these structures must have the same set of numbers T_1, T_2 and T_3, respectively. The structure with maximum $r^* = (y/x)_{\max}$ value, T_1^* T_2^* T_3^*; r^*, is filled up with *A* atoms in steps of $k = r^*, ...1, 0$ to complete occupation with *A* atoms at $y/x = 0$ (Hauck & Mika, 1994)

$$T_i(k) = T_i^{\max} - (T_i^{\max} - T_i^*)k/r^*,$$
$$y/x = k/(r^* + 1 - k).$$

These homologous series of structures also contain structures with $2k \leq r^*$ in Table 3 having *A* and *B* atoms interchanged,

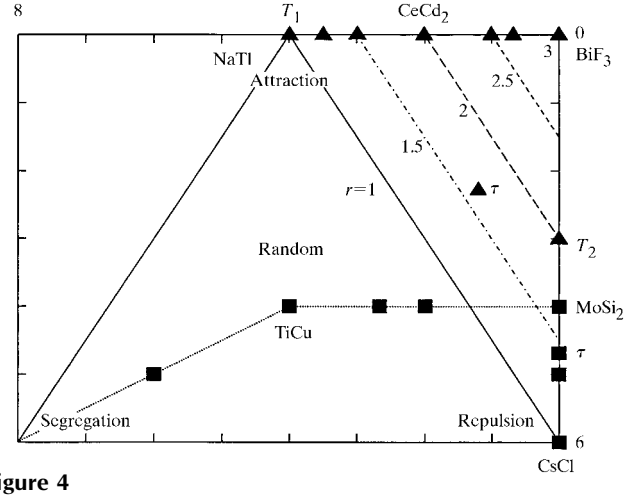

Figure 4
T_1, T_2 structure map of ordered b.c.c. A_xB_y compounds T_1 T_2 T_3; y/x for the [001] (■) and [111] (▲) layered compounds (Table 2*b*).

similar to $AuCu_3$ and $CuAu_3$ in the f.c.c. lattice (Hauck & Mika, 1994).

All structures of homologous series are usually at corners or edges of the structure map. In a few cases only the structures with maximum $r^* = (y/x)_{max}$ values are on the border (homologous II series, see §5). Other series of structures with identical unit cells are on the same border of the structure map with different α_i values (quasi-homologous structures).

The existence of homometric and homologous series of structures (with identical α_i values), as introduced above, shows that a single set of interaction parameters V_i can give rise to different structures. A final remark concerns homometric structures: these were not found in investigations of the Ising model (Ducastelle, 1991; Allen & Cahn, 1972; Finel & Ducastelle, 1984; Kanamori & Kakehashi, 1977).

Most of the observed crystal structures of ordered b.c.c. alloys (Parthé *et al.*, 1993) can be related to three different series of structures (Table 2*b*): The combination of 4 4 4; 1a and 0 6 12; 1 to give 2.7 4.7 6.7; 1 [Fig. 1A(*a*), deposited], the combination of 2 0 6; 2 and 0 3 9; 2 to give 0.7 2 8; 2 [Fig. 1A(*d*), deposited] and structures which can be considered as CsCl defect structures. Closely related structures with different composition were included within these series (Table 2*b*). For example, the Ti_2Cu_3 and Ti_3Cu_4 structures can be obtained by a combination of the $MoSi_2$ (0 4 4; 2) and γ-TiCu (4 4 4; 1) structures [Fig. 2A(*a*), deposited]. Au_2Nb_3 can be considered as a combination of 4 4 4; 2 and γ-TiCu (4 4 4; 1). Ti_3Pd_5 and Os_2Al_3 are combinations of $MoSi_2$ (0 4 4; 2) and CsCl (0 6 12; 1).

The 0 3 9; 2 structure is realised for $SiFe_2$ (HT) and Ti or Al atoms in the (Nb, Al)(Nb, Ti)Ti_2Al_2 structure [Fig. 2A(*b*), deposited]. The 2 0 6; 2 structure occurs for $CeCd_2$ or for $PbLi_2$, which is part of

Table 2

(*a*) Coordination T_1, T_2 and T_3 of A atoms and composition y/x in b.c.c..

A = W, Pa, Np (M^i = 1) and b.c.c. A_xB_y with single $T_i(A)$ and $T_i(B)$ values (M^i = 2, §2) (Fig. 1A, deposited) [homometric structures *a*, *b* are indicated by curly brackets, T_i; y/x values in brackets are not at the border of the structure map (Fig. 4)], coordination of A atoms and composition in square [or hexagonal (*)] planes, space group (SG) and Pearson symbol (PS), No. of reduced unit cell in Table 1A (deposited) and positions of atoms A_2–A_4 in addition to A_1 in the origin.

$T_i(A)$; y/x b.c.c.	$T_i(A)$; y/x square	SG	PS	No.	A_2	A_3	A_4
8 6 12; (1)	4 4 4; (1)	229	*cI*21	1			
(6 4 6; 1)†	2 2 0; 1	67	*oC*8	7	1 $\bar{1}$ 1		
(5 3 5; 1)†	1 2 4; 1	2	*aP*8	40	$\bar{1}$ 1 3	$\bar{2}$ 0 4	0 0 2
(4 4 4; 1a)† }	4 4 4; (1)	129	*tP*4	10	1 1 1		
(4 4 4; 1b)† }	2 0 4; 1	131	*tP*8	45	0 0 2	1 3 1	1 1 1
(4 3 4; 1)†	1 2 2; 1	11	*mP*8	46	1 $\bar{1}$ 3	1 1 1	0 0 2
(4 2 6; 1a) }	2 2 0; 1	11	*mP*4	8	0 $\bar{2}$ 2		
(4 2 6; 1b) }	2 2 0; 1	66	*oC*16	52	2 0 2	$\bar{1}$ 1 1	1 1 1
(4 2 5; 1)	1 2 4; 1	2	*aP*8	39	$\bar{2}$ 0 2	$\bar{1}$ $\bar{3}$ 3	0 $\bar{2}$ 2
(4 2 4; 1a)† }	2 0 4; 1	65	*oC*4	2			
(4 2 4; 1b)† }	2 0 4; 1	141	*tI*16	55	$\bar{1}$ $\bar{1}$ 1	1 $\bar{1}$ $\bar{1}$	2 0 0
(4 1 8; 1)†	0 4 4; 1	74	*oI*16	49	$\bar{1}$ 1 3	$\bar{1}$ 1 1	0 0 2
4 0 12; 1	0 4 4; 1	227	*cF*16	13	1 1 1		
(3 3 5; 1)†	1 2 4; 1	2	*aP*8	53	0 $\bar{2}$ 0	1 $\bar{3}$ $\bar{1}$	1 $\bar{1}$ $\bar{1}$
(2 4 6; 1)†	2 2 0; 1	74	*oI*8	12	0 0 $\bar{2}$		
0 6 12; 1	4 4 4; (1)	221	*cP*2	3			
(4 2 4; 1.3a) }	2 2 2; 1.3‡	2	*aP*7	31	1 $\bar{1}$ 1	2 $\bar{2}$ 0	
(4 2 4; 1.3b) }	2 2 2; 1.3‡	146	*hR*7	31	0 0 2	2 $\bar{2}$ 0	
(2 3 3; 1.5)	1 1 1; 1.5	12	*mC*10	17	1 $\bar{1}$ $\bar{1}$		
(4 2 2; 2a)† }	2 0 2; 2	69	*oF*12	4			
}	0 6 0; 2‡						
(4 2 2; 2b)† }	0 6 0; 2‡	151	*hP*9	58	0 0 2	1 $\bar{1}$ 1	
(2 2 2; 2)†	0 6 0; 2‡	2	*aP*9	66	0 $\bar{2}$ 2	1 $\bar{3}$ 1	
2 0 6; 2	6 6 6; (1)‡	164	*hP*3	5			
0 4 4; 2	4 4 4; (1)	139	*tI*6	6			
(3 1 2; 2.5)	1 1 1; 2.5‡	2	*aP*7	31	2 $\bar{2}$ 0		
2 0 0; 3	0 0 6; 3‡	166	*hR*4	9			
0 2 0; 4	0 0 0; 4	87	*tI*10	17			
2 0 0; 6	0 0 0; 6‡	148	*hR*7	31			

† On the borders of the T_1 T_2 T_3; y/x polyhedron. ‡ Hexagonal planar.

(*b*) Structures and $T_i(A)$ values of $A_xB_yC_z$ alloys (Fig. 2A, deposited) with sequences of layers AB (= *a*), ABB (= *b*) *etc*. A second space group is given for structures with higher SG than originally reported.

$A_xB_yC_z$		SG	PS	$T_i(A)$	$T_i(B)$	$T_i(C/D)$
W		229	*cI*2	8 6 12; (1)		
LT Pa		139	*tI*2	8 6 12; (1)		
β-Np		129/90	*tP*4	8 6 12; (1)		
α-Np		62	*oP*8	8 6 12; (1)		
Layered (001) structures (Schubert *et al.*, 1960) [Fig. 2A(*a*) deposited]						
CsCl	*a*(*AB*)	221	*cP*2	0 6 12; 1		
$MoSi_2$	*b*(AB_2)	139	*tI*6	0 4 4; 2		
$ReSi_2$	*b*	71	*oI*6	0 4 4; 2		
VAu_2	*b*	63/38	*oC*12	0 4 4; 2		
$AlAu_2$	*b*	62	*oP*12	0 4 4; 2		
AB_3	*c*(AB_3)	123	*tP*4	0 4 4; 3		
γ-TiCu	*d*(A_2B_2)	129	*tP*4	4 4 4; 1		
Au_2Nb_3	*e*(A_2B_3)	139	*tI*10	4 4 4; 1.5		
AB_2	*f*(A_2B_4)	129	*tP*6	4 4 4; 2		
AB	*g*(A_4B_4)	129	*tP*8	6 5 8; 1		
Ti_3Cu_4	*bd*	139	*tI*14	2.7 4 4; 1.3		
Ti_2Cu_3	*bdb*	129	*tP*10	2 4 4; 1.5		
Os_2Al_3	*ab*	139	*tI*10	0 5 8; 1.5		
Ti_3Pd_5	*bab*	123	*tP*8	0 4.7 6.7; 1.7		
ReAl(Re,Al)$_2$	*ACBC*	123	*tP*4	0 4 4; 3	0 4 4; 3	0 6 12; 1
Layered (111) structures (Zalkin & Ramsey, 1956) [Fig. 2A(*b*) deposited]						
CsCl	*h*(*AB*)	221	*cP*2	0 6 12; 1		
$CeCd_2$ ($PbLi_2$)	*k*(AB_2)	164	*hP*3	2 0 6; 2		
BiF_3, $AlFe_3$	*l*(AB_3)	225	*cF*16	0 0 12; 3		
AB_4	*m*(AB_4)	166	*hR*15	0 0 6; 4		

Table 2 (continued)

$A_xB_yC_z$		SG	PS	$T_i(A)$	$T_i(B)$	$T_i(C/D)$
AB_5	$n(AB_5)$	164	*hP*6	0 0 6; 5		
NaTl	$o(A_2B_2)$	227	*cF*16	4 0 12; 1		
Al_2Li_3	$p(A_2B_3)$	166	*hR*15	3 0 9; 1.5		
(AlLi)	$q(A_3B_3)$	164	*hP*6	4 2 8; 1		
Pb_2Li_7	*lm*	164/150	*hP*9	0 0 9; 3.5		
(Pb_4Li_{11})	*klll*	164	*hP*15	0.5 0 10.5; 2.75		
Pb_3Li_8	*lkl*	166	*hR*33	0.7 0 10; 2.7		
(Si_5Li_{13})	*lklkl*	164	*hP*18	0.8 0 9.6; 2.6		
Si_2Li_5	*kl*	166	*hR*21	1 0 9; 2.5		
$Zn(Ag,Zn)_2$	*k*	147	*hP*9	2 0 6; 2		
AB	*ho*	156	*hP*18	2.9 2 10.7; 1		
$SiFe_2$ HT	*hl*	164	*hP*6	0 3 9; 2		
$PtAl_2$	*hl*	164	*hP*12	0 3 9; 2		
Ga_4Li_5	*op*	164	*hP*9	3.5 0 10.5; 1.25		
$(AlLi_2)$	*lp*	164	*hP*9	2 0 10; 2		
$Ge_2Cu_2Li_5$	ABC_2BAC_3	164	*hP*9	0 0 9; 3.5	1 0 6; 3.5	
(Nb,Al)(Nb,Ti)Ti_2Al_2,	*ACDBDC*	164	*hP*6	0 0 6; 5	0 0 6; 5	0 3 9; 2
$Ni_2\square Al_3$	*ACACBC*	164	*hP*5	0 3 9; 2	0 0 6; 5	
SnMgLiPd	*ABCD*	216	*cF*16	0 0 12; 3	0 0 12; 3	0 0 12; 3
$AgSbLi_2$	*ABCC*	216	*cF*16	0 0 12; 3	0 0 12; 3	4 0 12; 3
$AlMnCu_2$	*ACBC*	225	*cF*16	0 0 12; 3	0 0 12; 3	0 6 12; 1
$VSnRh_2$	*ACBC*	139	*tI*8	0 0 12; 3	0 0 12; 3	0 6 12; 1
$USnPd_2$	*ACBC*	69/62	*oF*16	0 0 12; 3	0 0 12; 3	0 6 12; 1
CsCl related structures with composition of Cs/Cl layers [Figs. 2A(*a*) and (*b*) deposited]						
$Au(Zn,Au)_3$	A_2B_2/B_4	63/26	*oC*16	0 4 6; 3		
$(Mo,U)U_3$	AB/B_2	123	*tP*4	0 2 4; 3		
$Zn_3Ga_4Pd_7$	A_3B_4/C_7	146	*hR*42	0 2 4; 3.7	0 3 6; 2.5	0 6 12; 1
Pu_3Pd_4	A_6B/B_7	148	*hR*42	0 5 10; 1.3		
CsCl	*A*/*B*	221	*cP*2	0 6 12; 1		
UCo	*A*/*B*	199	*cI*16	0 6 12; 1		
RT AuCd	*A*/*B*	157	*hP*18	0 6 12; 1		
La(Ag,In)	*A*/*B*	139	*tI*16	0 6 12; 1		
δ-TiCu	*A*/*B*	123	*tP*2	0 6 12; 1		
RT PuGa	*A*/*B*	107	*tI*16	0 6 12; 1		
α-VIr	*A*/*B*	65	*oC*8	0 6 12; 1		
NaHg	*A*/*B*	63	*oC*16	0 6 12; 1		
Au(Cu,Zn)	*A*/*B*	55	*oP*8	0 6 12; 1		
Au(Zn,Au)	*A*/*B*	26	*oP*16	0 6 12; 1		
KHg	*A*/*B*	2	*aP*8	0 6 12; 1		
Other structures [Fig. 2A(*a*) deposited]						
Pb_5Li_{22}		216/196	*cF*432	0 0 4.8; 4.4		
In_3Li_{13}		227	*cF*128	0 0 4; 4.3		
Sb_2Tl_7		229	*cI*54	0 1 4; 3.5		
$AuMn_3$		123	*tP*12	0 2.67 4; 3		
Sn_3Li_7		11	*mP*20	0 3.3 4; 2.3		
$GaLi_2$		63	*oC*12	2 0 8; 2		
V_4Zn_5		139	*tI*18	4 3 4; 1.2		

the Pb_3Li_8 structure. The Pb_3Li_8, Al_2Li_3 and Si_2Li_5 structures can be divided in structural units similar to the 2 0 6; 2–0 3 9; 2 series [Fig. 2A(*b*), deposited]. CsCl is also a structural unit for combinations in the [111] direction (layers of Cs and Cl atoms, which alternate in the [111] direction).

The two families of structures with sequences of *A* or *B* atom layers in the [001] or [111] direction can be described by sequences of structural units *a* ($\widehat{=}$ layer sequence *AB*), *b* ($\widehat{=}$ layer sequence *ABB*) *etc.* (Table 2*b*), similar *e.g.* to the Ruddlesden–Popper and Aurivillius phases with sequences of *v* or *v*′ ($CaTiO_3$) and *w*′ (SrO) or *W*′ (WBi_2O_6) structural units, respectively (Hauck & Mika, 1997). The present families of structures are also named by the pioneers who investigated the crystal structures of the first example of the series: Au_2Nb_3 (Schubert *et al.*, 1960), Ti_2Cu_3 and Ti_3Cu_4 (Schubert *et al.*, 1964), Pb_2Li_7 (Zalkin & Ramsey, 1956) and Pb_3Li_8 (Zalkin *et al.*, 1956).

The $Zn_3Ga_4Pd_7$ and Pu_3Pd_4 structures of Fig. 2A(*b*) (deposited) are closely related to the CsCl (*AB*) structure, but with larger unit cells because of the different stoichiometry. Some of the *A* = Zn, Ga, Pu, Cs sites are occupied by *B* = Pd, Cl. A similar situation occurs for $AlFe_3$, $AlMnCu_2$ (Heusler alloy), $AgSbLi_2$ and SnMgLiPd [Fig. 2A(*a*), deposited]. The Sn, Mg, Li and Pd atoms of SnMgLiPd can be combined in five different ways to yield CsCl [(Sn,Mg)(Li,Pd)], $AlMnCu_2$ [$SnMg(Li,Pd)_2$], $AlFe_3$ [$Sn(Mg,Li,Pd)_3$], $AgSbLi_2$ [$LiSn(Mg,Pd)_2$] or NaTl [(Sn,Li)(Mg,Pd)]. The combination is similar to the sphalerite-related structures (Hauck & Mika, 1998*a*) or the combination of two 0 0 4; 3 square layers to give 0 4 4; 1 (Fig. 1) as was outlined in step (ix), §1.

The sequence Ni Al Ni Al □ Al of vacancies □ = *B* in the $Ni_2\square Al_3$ structure (*ACACBC*) (Table 2*b*) can alternate in a sequence of Fibonacci numbers, if the composition is varied to $Ni_{1.85}\square_{1.15}Al_3$ (Chattopadhyay *et al.*, 1987).

The structures of Po (§5) and diamond have the same $T_i(A)$ values as CsCl (□Po) and NaTl (□C), respectively, with vacant Cs or Na positions. The number of vacancies □ is increased to 432 − 58 = 374 in an idealized α-Mn (0 0 1.24; 6.45) with the *x*, *y*, *z* parameters of the 58 Mn atoms 1/3 (*w* = 0.317, *u* = 0.356), 1/4 (*v*′ = 0.278), 1/12 (*u*′ = 0.089) and 0 (*v* = 0.042) rather than the observed values in brackets (Wyckoff, 1982).

The metal atoms of the idealized superconducting oxides (Hauck & Mika, 1997, 1998*b*) lie on a b.c.c. lattice with structures similar to the Schubert family. The metal lattices of $CuLa_2O_4$ and $LaCu_2La_2O_7$ correspond to $MoSi_2$ and Os_2Al_3 ($AlOs_2Al_2$; Table 2*b*). The formulae Cu′La_2O_4, La′$Cu_2La_2O_7$ and Cu′$Ba_2Cu_2Y'O_7$ (instead of La_2CuO_4, $La_3Cu_2O_7$ and $YBa_2Cu_3O_7$) show the sequence of metal atoms Cu′LaLa, La′CuLaLaCu and Cu′BaCuY′CuBa with a single Cu′, La′ and Y′ at mirror planes and two other atoms left and right of the mirror plane.

4. Face-centered cubic alloys A_xB_y

The face-centered cubic structure is obtained if spheres with diameter d are ordered with the cubic close-packed structure. The distance between two identical square layers of the face-centered Cu structure $a_0 = 2^{1/2}d$ can be increased up to $1.66d$ in In, Ga, La or Ce, or decreased to $1.33d$ in Pu or $1.0d$ in W (Wyckoff, 1982; Ho & Douglas, 1968; Pearson, 1972; Villars & Calvert, 1986; Hyde & Andersson, 1989; Parthé *et al.*, 1993). The undistorted structures are compared in the present paper using the self-coordination numbers T_i of b.c.c. and f.c.c. alloys and their different locations on structure maps.

The 28 structures of ordered f.c.c. A_xB_y with single $T_1\ T_2\ T_3$; y/x values (M^i = 2, §2) are listed in Table 4(*a*). 15 of these structures are at the corners of the structure map (Fig. 5). Only seven structures were obtained by the Ising model (Kanamori & Kakehashi, 1977). The 12 6 24; (1), 6 0 12; 1a,b, 4 4 16; 1 and 4 6 8; 1 structures are the limiting structures at $y/x = 1$ (Fig. 5). 6 0 12; 1a,b, 5 3 12; 1a,b and 4 2 12; 1.3a,b are homometric structures – structures with identical T_i values, but different symmetry as was outlined in §3. Other structures such as 2 2 12; 2a,b,c are 'quasi-homometric' with some deviations of higher T_i values. The lattice energies of the undistorted lattices as given by the Madelung factors are slightly different (Hauck *et al.*, 1988*b*,*d*).

The 0 6 0; 3 $AuCu_3$, 4 6 8; 1 CuAu, 2 2 12; 2a $MoPt_2$ and 0 2 8; 4 $MoNi_4$ structures are within homologous series of structures with identical α_i values (Table 5), as was outlined for b.c.c. alloys in §3.

Three different series of experimental structures are shown in Figs. 3A(*a*)–(*c*) (deposited). The compilation (Table 4*b*) also includes some theoretical structures and some NaCl (Hauck *et al.*, 1988*c*) or ZnS (Hauck & Mika, 1998*a*) derivative structures, which are shown in Figs. 3A(*a*)–(*d*) (deposited), if the corresponding structures of alloys are not known. The Na and Cl atoms of the NaCl structure form two f.c.c. lattices with a translation $a_0/2$, $a_0/2$, $a_0/2$ of the lattice constant a_0. The f.c.c. lattices of ZnS (sphalerite) are translated by $a_0/4$, $a_0/4$, $a_0/4$. The ordering of metal atoms at Na or Zn positions or non-metal atoms at Cl or S positions can be characterized by the s-CN values T_i similar to alloys. In α-$NaFeO_2$, *e.g.* the Na and Fe atoms occupy the same positions as the Cu and Pt atoms in CuPt,a (Table 4*b*). The corresponding ZnS derivative structure is In(Ga,Al)P_2 with a disordered distribution of Ga and Al atoms at the Pt positions of the CuPt structure. In Cd□Cl_2 and Gd_2□C the Cd atoms and vacancies □ or the C atoms and vacancies form the CuPt structure. In □Nb_3□O_3 the metal □Nb_3 and non-metal sublattices □O_3 are both ordered as in the $AuCu_3$ structure. The space group number and Pearson symbol listed in Table 4(*b*) correspond to the compounds $A_xB_yC_z$.

The T_1 and T_2 values in the $T_1\ T_2\ T_3$; y/x notation of NaCl-related compounds describe the connection of octahedra by edges and corners, respectively. For example, the 1 0 7; 4 UCl_5 structure contains UCl_6 octahedra connected by one edge to form $(UCl_5)_2$, while the UF_6 octahedra of 0 2 8; 4 UF_5 are connected by two corners in a one-dimensional row. The CTi_6 octahedra of 6 0 12; 1b Ti_2C are linked by six edges, the NTi_6 octahedra of 4 4 16; 1 Ti_2N are linked by four edges and four corners. The vacancies □ of 0 0 8; 5 V_6C_5□ or the Re atoms of 0 0 8; 5 Li_5ReO_6 form isolated octahedra. Usually the metal atoms with high valency such as U^{5+} or Re^{7+} are as far apart as possible with low T_1 and T_2 values because of repulsive interactions.

Table 3
s-CN values of some homologous series of b.c.c. derivative structures (Fig. 1A, deposited) with different r and k values (see text).

r^*	k	$T_i(A)$
6	6	2 0 0; 6
6	5	3 1 2; 2.5
6	4	4 2 4; 1.33a,b
6	3	5 3 6; 0.75a,b
6	2	6 4 8; 0.4
6	1	7 5 10; 0.17
6	0	8 6 12; (0)
4	4	0 2 0; 4
4	3	2 3 3; 1.5
4	2	4 4 6; 0.67
4	1	6 5 9; 0.25
4	0	8 6 12; (0)
3	3	2 0 0; 3
3	2	4 2 4; 1a,b
3	1	6 4 8; 0.33
3	0	8 6 12; (0)

The number T_1 of nearest neighbors of ZnS derivative structures corresponds to the number of ZnS_4 tetrahedra shared by corners. In *e.g.* $(Ni, Cu)_5Si_2S_7$ with an ordering of Si atoms as in the Mn_2Au_5 alloy (1 3 10; 2.5), each SiS_4 tetrahedron is linked to another SiS_4 tetrahedron in Si_2S_7 groups.

Pauling's electrovalence rule is satisfied for all NaCl derivative structures with composition $r = y/x = 1$, 2 and 5 along the upper right-hand border of the structure map with $T_2 = -2T_1 + 6(3 - r)$ for $1 \le r \le 2$ and $T_2 = -2T_1 + 2(5 - r)$ for $2 \le r \le 5$, and for all ZnS derivative structures with composition $r = y/x = 1$ and 3 along the right-hand border ($T_1 = 6 - 2r$; Hauck & Mika, 1994, 1998*a*). The Ti atoms of Ti_2C□ (6 0 12; 1a structure) and Ti_2N□ (4 4 16; 1 structure) at the two ends of the $T_2 = -2T_1 + 12$ line are surrounded by three C atoms in a facial configuration in Ti_2C and three N atoms in a meridional configuration in Ti_2N, because of the different interaction energies between these atoms.

The carbides Ti_2C, Gd_2C, Ti_8C_5, V_6C_5 and V_8C_7 are located at low T_2 values of the structure map, indicating covalent-type bonding, while the nitrides Ti_2N, Nb_4N_3 and the hydrides Pd_2H, Pd_5D_4 are located at increased T_2 values, indicating Coulomb-type interactions (Table 4*b*; Hauck & Mika, 1994).

The N atoms of Ti_2N are further apart than the C atoms of Ti_2C and are stabilized by Coulomb interactions with a Madelung factor increased by 1.9%. The Ti_2C structure is stabilized by covalent forces with a slight reduction in the length of all Ti—C bonds (Hauck & Mika, 1994). A similar situation exists for a *cis* configuration of the Sn atoms in

Li_2SnO_3 (3 0 10; 2b) or mixed *cis* and *trans* configuration of Zr atoms in Li_2ZrO_3 (2 2 12; 2a). (The O atoms occupy all Cl positions of the NaCl structure.) A structure with all Zr atoms in *trans* configurations is not possible in NaCl derivative structures. At $y/x = 5$, as *e.g.* in Li_5ReO_6 or $V_6C_5\square$, isolated ReO_6 or $\square V_6$ octahedra are formed with one Re atom (or $\square$) next to each O (or V) atom.

The limiting structures 0 6 0; 3, 0 4 8; 3, 4 6 8; 1 and 4 4 16; 1 can be split into structural units *u*, *v*, *x* and *y*, which can be combined like the parts of a puzzle to obtain the crystal structures found at the right-hand border [Fig. 3A(*c*), deposited]. The *u*′, *v*′, *x*′ and *y*′ units are obtained from the *u*, *v*, *x* and *y* structural units by the translation $a_0/2$, $a_0/2$, 0.

The structures with a single environment of *A* atoms can be characterized by square or hexagonal layers with small unit cells, as shown in Table 4(*a*), and one or two structural units such as *x* (CuAu) or *xy*′*x*′*y* (UPb) [Fig. 3A(*c*), deposited]. The *x*′*y* structural units can be obtained by a shearing of the *xy*′ units with the translation $a_0/2$, $a_0/2$, 0. Structures containing several related structural units such as yx_9 and $y'x'_9$ in CuAu II with the sequence $yx_9y'x'_9$ [Fig. 3A(*c*), deposited] are considered as shear structures with antiphase boundaries between yx_9 and $y'x'_9$ (Schubert, 1964; Sato & Toth, 1965; Hyde & Andersson, 1989). Other structures of Fig. 3A(*c*) (deposited) such as $ZrGa_2$ exhibit a symmetrical sequence of structural units (*vyuuyv*).

The observed structures (Table 4*b*) as *e.g.* the CuAu II or $ZrAl_3$ structure at the right-hand boundary of the structure map (Fig. 5) consist of *u*, *v*, *x*, *y* structural units, which are connected by 0 4 4; 1 square planes (Fig. 1). The other layers of the CuAu–UPb and $AuCu_3$–$TiAl_3$ parent structures do not fit together. The structural units of many structures on the right-hand side of the structure map (Fig. 5) are connected by 2 0 4; 1 or 0 4 4; 1 square planes (Table 4*a*). The (theoretical) structures on the left-hand side of the structure map are connected by 6 6 6; (1) hexagonal planes (Hauck & Mika, 1994). $Al_2\square_2C_3$ (*ac*′) (Ketelaar, 1935; Ketelaar *et al.*, 1947), Mo_3Al_8 (gh_2) (Forsyth & Gran, 1962), CuAu II ($yx_9y'x'_9$) (Johansson & Linde, 1936) and $ZrAl_3$ ($v_4v'_4$) (Brauer, 1939) are the first structures of the three structure families (Table 4*b*).

The AB_3 structures such as $TiAl_3$ ($u_2u'_2$) or $ZrAl_3$ ($v_4v'_4$) (Brauer, 1939) are obtained from *u* and *v* units and the *AB* structures such as $yx_9y'x'_9$ (CuAu II) (Johansson & Linde, 1936) from a combination of the *x* and *y* structural units. The structures with intermediate composition such as AB_2 are obtained by combination of *u*, *v*, *x* and *y* units [Table 4*b*, Fig. 3A(*c*), deposited]. The NaCl-related structures at the right-hand border of the structure map contain vacancies in the structural units to approach Pauling's electrovalence rule such as u_2 for $\square Nb_3\square O_3$ (NbO), $v'xu_2xv'$ for $V_2\square_4O_5\square$ (V_2O_5), $uxv'x'u'$ for $Mo_2\square O_3$ (MoO_3), $u_2xv'_4xu_2$ for $Nb_3\square_7FO_7\square_2$ (Nb_3O_7F), xv'_2xu_2 for $Nb_2\square_4O_5\square$ (*R*-Nb_2O_5) or the two-dimensional shear structures of *e.g.* (Au,Zn)Cu_3, $ZnAu_3$ (Schubert, 1964; Sato & Toth, 1965), $(W_{0.2}V_{0.8})_9\square_{16}O_{21}\square_4$ $[(W_{0.2}V_{0.8})_3O_7]$ or $Nb_{16}\square_{33}O_{40}\square_9$ (*M*-Nb_2O_5; Hyde & Andersson, 1989). The two-dimensional shear structures, however, are not at the border of the structure map and contain different structural elements [hatched areas in Fig. 3A(*d*), deposited]. Non-periodic antiphase boundaries in two dimensions were observed in $ZnAu_3$ (Teuho *et al.*, 1987).

Some of the remaining observed structures (Table 4*b*) can be classified in a similar way to the three structure families of ordered b.c.c. structures (Table 2*b*). The square layers of *A*

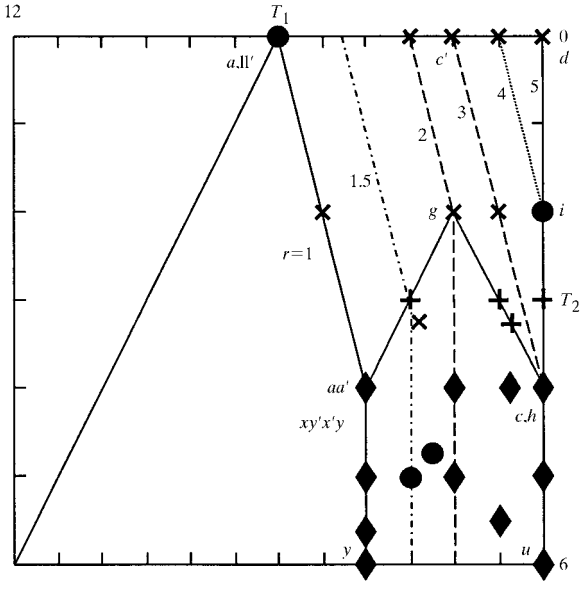

Figure 5
Structure map of ordered f.c.c. A_xB_y alloys with s-CN values of *A* atoms as parameters and structural units *a*–*y*. The boundary of the structure map is outlined for $r = y/x$ by differently dashed lines. The T_1 and T_2 values of the Johansson & Linde and Brauer (♦), Ketelaar (×) and Forsyth & Gran families (+) and the [001] (■) or [111] (▲) layered structures are in different areas of the structure map.

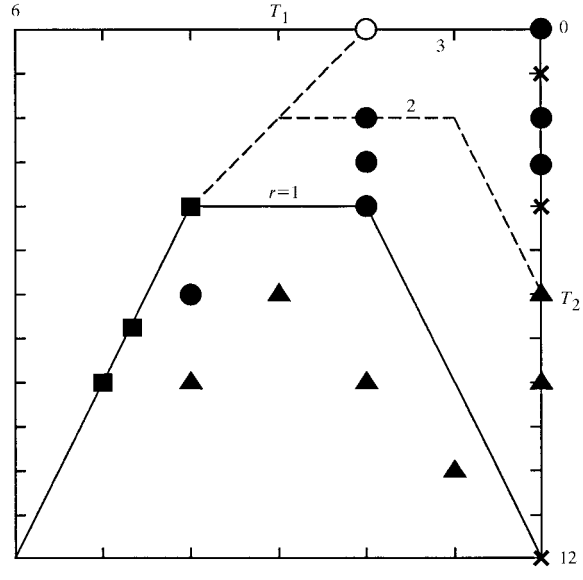

Figure 6
T_1, T_2 structure map of the p.c. lattice with [001] (■), [110] (●), [111] (▲) layered, ZnS related (×) and other (○) compounds in different areas.

atoms perpendicular to the drawing plane are separated by layers of B atoms in TiCd and $CuZr_2$ similar to γ-TiCu and $MoSi_2$ (Table 2*b*). These compounds with T_i values 8 4 8; 1 (TiCd) and 4 4 0; 2 ($CuZr_2$), which are not at the border of the f.c.c. structure map (■) (Fig. 5), should be considered as distorted γ-TiCu or $MoSi_2$ with the same space groups and Pearson symbols. Most of the observed structures are at boundary lines for the given composition. The only exceptions in Table 4(*b*) are $\square_4Co_5Ge_7$ and V_4Zn_5, which should be reinvestigated after extended annealing to avoid a partial disorder which is inherent in all structures inside the structure map.

5. Primitive cubic lattice

The crystal structure of α-Po has a primitive-cubic (p.c.) structure (Galasso, 1970; Donohue, 1974). More important are the CaF_2 derivative structures (Fig. 3) (Müller, 1991; Juza *et al.*, 1959). The Ca and F atoms form f.c.c. and p.c. structures, respectively, but only the F lattice is considered here. Some compounds with CaF_2 structure such as CeO_2, PrO_2 or TbO_2 can form oxygen-deficient structures, *e.g.* Pr_nO_{2n-2}, where n = 7, 9, 10, 11, 12, and some of the oxygen positions are vacant (Schweda *et al.*, 1991; Zhang *et al.*, 1993, 1995*a*,*b*, 1996). These compounds and the anions of PbO, PtS and Cu_2O can be described as p.c. compounds A_xB_y with A = vacancy (□) and B = O or S and metal atoms Pb, Pt, Cu at Ca positions of CaF_2. The other compounds shown in Fig. 4A (deposited) are derived from the antifluorite structure of Li_2O with an ordered distribution of metal atoms such as β-$Li_5Al\square_2O_4$ (Stewner &

Table 4

(*a*) Cubic close-packed alloys A_xB_y with single $T_i(A)$ and $T_i(B)$ values characterized by the s-CN values T_i of A atoms in a c.c.p. structure and in square planes (only occupied planes perpendicular to the direction with the highest symmetry are included), space group (SG), Pearson symbol (PS), No. of reduced cells (Table 2A, deposited) and positions of atoms A_2–A_4.

$T_i(A)$; *y*/*x* c.c.p.	$T_i(A)$; *y*/*x* square	SG	PS	No.	A_2	A_3	A_4
12 6 24; (1)	4 4 4; (1)	225	*cF*4	1			
9 3 12; 1	6 6 6; (1)†	166	*hR*4	7	1 0 1		
(8 4 8; 1)‡	4 4 4; (1)	129	*tP*4	8	0 1 1		
(7 2 10; 1)‡	3 2 2; 1	11	*mP*8	43	0 1 1	1 0 1	1 $\bar{1}$ 2
(6 2 12; 1a)	2 0 4; 1	59	*oP*4	9	0 1 1		
(6 2 12; 1b)	2 0 4; 1	131	*tP*8	47	0 $\bar{1}$ 1	1 0 1	1 1 2
(6 1 12; 1)	2 0 4; 1	11	*mP*8	41	0 1 1	1 0 3	0 0 2
6 0 12; 1a	2 0 4; 1	166	*hR*2	2			
6 0 12; 1b	2 0 4; 1	227	*cF*32	53	1 1 0	0 1 1	1 0 1
(5 4 10; 1)	1 2 2; 1	11	*mP*8	48	1 2 1	1 0 1	0 1 1
(5 3 12; 1a)	3 2 2; 1	12	*mC*8	10	0 0 2		
(5 3 12; 1b)	2 2 2; 1	15	*mC*16	52	2 0 0	3 $\bar{1}$ 0	1 0 $\bar{1}$
5 2 14; 1	1 2 2; 1	15	*mC*16	51	$\bar{1}$ $\bar{1}$ 2	$\bar{1}$ 0 1	0 $\bar{1}$ 1
4 6 8; 1	4 4 4; (1)	123	*tP*2	3			
4 5 12; 1a	0 4 4; 1	74	*oI*16	45	0 $\bar{1}$ 3	0 $\bar{1}$ 1	0 0 2
4 4 16; 1	0 4 4; 1	141	*tI*8	13	0 $\bar{1}$ 1		
4 2 12; 1.3a	2 2 2; 1.3†	2	*aP*7	34	1 $\bar{1}$ 0	0 $\bar{1}$ 1	
4 2 12; 1.3b	2 2 2; 1.3†	146	*hR*7	34	1 $\bar{2}$ 1	1 $\bar{1}$ 0	
3 3 12; 1.5	1 1 1; 1.5	12	*mC*10	18	1 0 1		
6 0 6; 2	6 6 6; (1)†	164	*hP*3	4			
(4 4 0; 2)‡	4 4 4; (1)	139	*tI*6	5			
2 2 12; 2a	2 0 2; 2	71	*oI*6	6			
2 2 12; 2b	0 6 0; 2†	151	*hP*9	62	1 $\bar{1}$ 0	1 $\bar{2}$ $\bar{1}$	
2 2 12; 2c	0 6 0; 2†	2	*aP*6	63	3 $\bar{1}$ 0	2 $\bar{1}$ 1	
2 1 9; 2.5	1 1 1; 2.5†	2	*aP*7	34	0 $\bar{1}$ 1		
0 6 0; 3	0 4 4; 1	221	*cP*4	12			
0 2 8; 4a	0 0 0 4; 4	87	*tI*10	18			
0 0 6; 6	0 0 0 6; 6†	166	*hR*7	34			

† Hexagonal planar. ‡ On the borders of the T_2 T_2 T_3; *y*/*x* polyhedron.

(*b*) Structures and $T_i(A)$ values of $A_xB_yC_z$ alloys, and corresponding NaCl and ZnS derivative structures within different series of structural units and other structures [Figs. 3A(*a*)–(*d*), deposited, see text].

$A_xB_yC_z$	SG	PS	$T_i(A/B/C)$	NaCl derivative	ZnS derivative
Cu	225	*cF*4	12 6 24; (1)	NaCl	ZnS
α-Hg	166	*hR*1	12 6 24; (1)	NiO	
Al,Zn metast.	166	*hR*1	12 6 24; (1)		
Pr HP	152	*hP*6	12 6 24; (1)		
In	139	*tI*2	12 6 24; (1)	CoO	
γ-Mn	139	*tI*2	12 6 24; (1)		
α''-Ce I	12	*mC*2	12 6 24; (1)		
α''-Ce II	12	*mC*4	12 6 24; (1)		
Cf HP	2	*aP*4	12 6 24; (1)		
[110] structural units *a*–*d*, *k*, *l* of Ketelaar (1935), Ketelaar *et al.* (1947) family [Fig. 3A(*a*), deposited]					
CuPt,a	*a*	166	*hR*2	6 0 12; 1a	α-$NaFeO_2$, Gd_2C,$CdCl_2$	In(Ga,Al)P_2
CuPt,b	*l l′*	227	*cF*32	6 0 12; 1b	$LiTbS_2$, Ti_2C,ZrS_2	
AB	a_2a_2'	66	*oC*16	5 2 14; 1a	$NaDyO_2$	
AB	a_3a'	15	*mC*16	5 2 14; 1b		
AB	*bb′*	67	*oC*16	5 3 14; 1		
UPb	*aa′*	141	*tI*8	4 4 16; 1	Pd_2D,Ti_2N	$CuFeS_2$
AB	*b*	131	*tP*8	4 5 12; 1b		
$(Zn, Ga)_3Au_5$	*bcb′c*	72	*oI*32	2.7 3.3 10.7; 1.7		
A_3B_5	*kk′*	166	*hR*8	4 0 8; 1.7	Ti_8C_5	
AB_2	*ac′*	12	*mC*12	3 0 10; 2b	$AlCl_3$,Li_2SnO_3	
AB_2	*ac′a′c′*	70	*oF*48	3 0 10; 2c	Sc_2S_3,$CrCl_3$	
AB_2	*ca′*	15	*mC*12	2 2 12; 2d	Li_2ZrO_3,III	
AB_2	*aca′c*	70	*oF*48	2 2 12; 2f		
$CuPt_3$	*c′*	65	*oC*8	2 0 4; 3	$OsCl_4$,Tm_3Se_4	
AB_3	*ad′*	15	*mC*16	2 0 8; 3a		
AB_3	*adad′*	15	*mC*32	2 0 8; 3b		
AB_3	*ada′d*	15	*mC*32	2 0 8; 3c		

Table 4 (continued)

$A_xB_yC_z$		SG	PS	$T_i(A/B/C)$	NaCl derivative	ZnS derivative
AB_3	*ad*	13	*mP*8	2 0 8; 3e	$ZrCl_4$	
AB_3	*cc′*	69	*oF*32	1 2 6; 3		
$TiAl_3$	*c*	139	*tI*8	0 4 8; 3	Nb_4N_3,SnF_4	$SbCu_3S_4$
AB_4	*c′dc′d′*	70	*oF*40	1 0 6; 4c		
AB_4	*c′d*	12	*mC*20	1 0 6; 4d	K_4UO_5	
AB_4	*cdcd′*	70	*oF*80	0 2 8; 4b		
AB_4	*dc*	15	*mC*20	0 2 8; 4c	M_4UO_5	
AB_5	*dd′*	70	*oF*48	0 0 8; 5a	Lu_5S_6	
AB_5	*d*	12	*mC*12	0 0 8; 5e	V_6C_5(I),Sc_5S_6 β-Li_6UO_6	
[210] structural units *e–i* of Forsyth & Gran (1962) family [Fig. 3A(*b*), deposited]						
UPb	*eg*	141	*tI*8	4 4 16; 1	Pd_2D,Ti_2N	$CuFeS_2$,α-$ZnCl_2$
CuAu	*f*	123	*tP*2	4 6 8; 1		(Ga,As)(Al,As)
NaHg	*f*	63	*oC*16	4 6 8; 1		
A_2B_3	*eh*	12	*mC*10	3 3 12; 1.5		
$MoPt_2$	*ef*, *g*	71	*oI*6	2 2 12; 2a	$\square Ti_2\square O_2$	$GeCu_2Se_3$
AB_2	*fh*	12	*mC*12	2 4 6; 2		
AB_2	*ei*	12	*mC*12	3 2 8; 2		
Mn_2Au_5	*gh*	12	*mC*14	1 3 10; 2.5		$NiSi_2Cu_4S_7$
A_2B_5	*fi*	12	*mC*14	2 3 6; 2.5		
Mo_3Al_8	gh_2	12	*mC*22	0.7 3.3 9.3; 2.7		
AB_3	*gi*	12	*mC*16	1 2 10; 3		
$TiAl_3$	*h*	139	*tI*8	0 4 8; 3	Nb_4N_3, SnF_4	$SbCu_3S_4$
A_2B_7	*hi*	12	*mC*18	0 3 8; 3.5		
$MoNi_4$	*i*	87	*tI*10	0 2 8; 4a	UF_5,Na_4UO_5, Pd_5D_4,Ti_4O_5	
[001] structural units *u–y* of Johansson & Linde (1936) and Brauer (1939) family [Fig. 3A(*c*) deposited]						
UPb	$xy'x'y$	141	*tI*8	4 4 16; 1	γ-$LiFeO_2$, Pd_2D,Ti_2N	$CuFeS_2$
CuAu II	$yx_9y'x'_9$	74	*oI*40	4 5.6 9.6; 1		
CuAu	*x*	123	*tP*2	4 6 8; 1		(Ga,As)(Al,As)
NaHg	*x*	63	*oC*16	4 6 8; 1		
$ZrSi_2$	$uu'y'v'vy$	63	*oC*12	2 4 8; 2a		
$(Zr,Al)(Si,Al)_2$	$uu'x'vv'y'$ $u'uxv'vy$	141	*tI*24	2 4 8; 2b		
$ZrGa_2$	v_2yu_2y	65	*oC*12	2 5 4; 2a		
$HfGa_2$	u_2yv_2x' $u'_2y'v'_2x$	141	*tI*24	2 5 4; 2b		
Nb_5Ga_{13}	$uu'_2uyvv'_2v_2$ $v'_2vyuu'_2u$	65	*oC*36	0.8 4 8; 2.6		
$TiAl_3$	$u_2u'_2$	139	*tI*8	0 4 8; 3	Nb_4N_3,SnF_4	$SbCu_3S_4$
$ZrAl_3$	$v_4v'_4$	139	*tI*16	0 5 4; 3		
$CdAu_3$ II	$v_4v'_4$	107	*tI*16	0 5 4; 3		
$AuCu_3$	*u*	221	*cP*4	0 6 0; 3	$\square Nb_3\square O_3$,	$\square CdIn_2Se_4$
SiU_3-tetr.	*u*	140	*tI*16	0 6 0; 3		
$SiIr_3$	*u*	140	*tI*16	0 6 0; 3		
LT $GaPt_3$	*u*	127	*tP*16	0 6 0; 3		
$SrPb_3$	*u*	123	*tP*4	0 6 0; 3		
$CuTi_3$	*u*	123	*tP*4	0 6 0; 3		
SiU_3-orth.	*u*	69	*oF*32	0 6 0; 3		
$GePt_3$	*u*	12	*mC*16	0 6 0; 3		
$PdAuCu_2$	*u*	123	*tP*4	0 6 0; 3/ 0 6 0; 3/ 4 6 8; 1		
$ZnAu_3$	*u*	142	*tI*64	0 6 0; 3		
(Tl,Pb)Pd_3	*u*	139	*tI*24	0 6 0; 3		
α-$PdCu_3$	*u*	123	*tP*28	0 6 0; 3		
$(Pt,Zn)(Zn,Cu)_3$	*u*	139	*tI*40	0 6 0; 3		
$(Zn,Ga)Au_3$	*u*	140	*tI*48	0 6 0; 3		
Ce_3Sn_7	u_4yv_4y	65	*oC*20	1.3 5.3 2.7; 2.3		
Gd_3Sn_7	u'_2uyv v'_2vyu	65	*oC*20	1.3 4 8; 2.3		
Ce_2Sn_5	$v'_6y'u'_6y'$	65	*oC*28	1 5.5 2; 2.5		
Layered (001) structures						
CuAu	(*AB*)	123	*tP*4	4 6 8; 1		(Ga,As)(Al,As)
$CuZr_2$	(AB_2)	139	*tI*6	4 4 0; 2		$(Ga,As)(Al,As)_2$
TiCd	(A_2B_2)	129	*tP*4	8 4 8; 1		$(Ga,As)_2(Al,As)_2$

Hoppe, 1971*a*), β-$Li_5Ga\square_2O_4$ (Stewner & Hoppe, 1971*b*), $Li_5Tl\square_2O_4$ (Hoppe & Panek, 1971) or $Na_6Pb\square O_4$ (Panek & Hoppe, 1973).

There were 36 structures with a single environment T_i of *A* and a single environment T_i of *B* atoms (M_i = 2, §2) obtained in the present investigation (Table 6*a*). The structure map of the p.c. lattice (Fig. 6) is similar to the structure map of $CaTiO_3$ related structures (Hauck & Mika, 1997, 2000*a*), but different from the structure maps of the square, b.c.c. or f.c.c. lattice (Figs. 2, 4 and 5). The maximum range of the Cowley short-range order parameters α_i (i = 1–3) is obtained for a tetrahedron with the four structures 0 12 0; 1, 2 4 8; 1, 4 4 0; 1 and 6 12 8; (1) at the corners. A 3 0 T_3; 1 structure (α_1 = 0, α_2 = −1) for covalent bonding is impossible in the p.c. lattice. The lowest T_2 = 4 value is obtained in Pb□O (4 4 0; 1) and Pt□S (2 4 8; 1) with y/x = 1. At y/x = 3, T_2 = 0 is reached in $Si\square_3S_2$ (2 0 0; 3) and $Cu_2\square_3O$ (0 0 8; 3). The highest T_2 = 12 value in ZnS (0 12 0; 1) indicates a repulsion of Zn atoms. The s-CN values T_1 and T_2 give the numbers of ZnS_4 tetrahedra, which are linked by edges and corners, respectively. In the f.c.c. system T_1 was the number of linked corners; a connection by edges is not allowed in the f.c.c. system (§4). The combination of structural units at the boundary of the structure map was outlined in some detail (Hauck & Mika, 1997, 2000*a*).

Most observed structures are within two structure series of (110) layered structures and the ZnS family (Tables 6*b* and *c*). The ZnS (sphalerite) related structures are listed already in Table 4(*b*) because of the two f.c.c. lattices of Zn and S atoms with a translation of $a_0/4$, $a_0/4$, $a_0/4$. Many structures can be considered as combinations of

Table 4 (continued)

$A_xB_yC_z$		SG	PS	$T_i(A/B/C)$	NaCl derivative	ZnS derivative
Layered (111) structures						
CuPt, a	(AB)	166	$hR2$	6 0 12; 1a	α-$NaFeO_2$	In(Ga,Al)P_2
$ZnAl_2$	(AB_2)	164	$hP3$	6 0 6; 2	In_2S_3	
AB	(A_2B_2)	166	$hR4$	9 3 12; 1		
CuAu (CsCl) related structures in [001] projection with composition of Cu/Au layer						
Ti_2Ga_3	A_4B/B_5	83	$tP10$	3 5 6; 1.5		
AB_3	AB/B_2	65	$oC4$	2 2 4; 3a		
$PdCu_4$	A_2B_3/B_5	84	$tP20$	1 1 4; 4		
$\square_4Co_5Ge_7$	B_5C_3/ A_4C_4	107	$tI24$	2 2 4; 3/ 1.6 4.8 3.2; 2.2/ 4.6 2.7 9.1; 1.3		
CuPt (CsCl) related structures in [111] projection with composition of Cu/Pt layer						
AB_2	A_2B/B_3	15	$mC24$	3 0 10; 2a	$TiCl_3$, β-Na_2PtO_3	
AB_5	AB_2/B_3	151	$hP18$	0 0 8; 5f	V_6C_5(II), Li_5ReO_6	
AB_5	AB_2/B_3	15	$mC24$	0 0 8; 5b	V_6C_5(III)	
AB_5	AB_2/B_3	12	$mC12$	0 0 8; 5e	$\square Sc_5S_6$	
Other compounds						
AB		59	$oP4$	6 2 12; 1a		
AB		131	$tP8$	6 2 12; 1b		
AB_2		151	$hP9$	2 2 12; 2e		β-Ga_2Se_3
AB_3		63	$oC16$	2 2 4; 3b		
AB_3		15	$mC32$	2 0 8; 3d	Hf I_4	
AB_4		14	$mP20$	1 0 7; 4a	UCl_5	
AB_7		212	$cP32$	0 0 6; 7	V_8C_7	
V_4Zn_5		139	$tI18$	5 4 6; 1.25		
Mn_7Pd_9		139	$tI32$	3.4 5.1 6.9; 1.3		
Zn_3Au_5		72	$oI128$	2.7 3.7 9.3; 1.7		
Ga_3Pt_5		65	$oC16$	2.7 4.7 5.3; 1.7		
$Mn_{11}Pd_{21}$		123	$tP32$	2.2 4.4 4.4; 1.9		
Mn_9Au_{31}		83	$tP40$	0 3.3 7.1; 3.4		
$GeCa_7$,$CuPt_7$		225	$cF32$	0 0 0 12; 7		
$TiPt_8$		139	$tI18$	0 2 0; 8		

Table 5
s-CN values of some homologous series of f.c.c. derivative structures with different r and k values (see text).

r^*	k	T_i(A)	Prototype
2	2	2 2 12; 2a	$MoPt_2$
2	1	7 4 18; 0.5a	Pt_2Mo
2	0	12 6 24; 0	Cu
3	3	0 6 0; 3	$AuCu_3$
3	2	4 6 8; 1	AuCu
3	1	8 6 16; 0.33	Cu_3Au
3	0	12 6 24; 0	Cu
4	4	0 2 8; 4	$MoNi_4$
4	3	3 3 12; 1.5	
4	2	6 4 16; 0.67	
4	1	9 5 20; 0.25	Ni_4Mo
4	0	12 6 24; 0	Cu

$SbCu_3S_4$ ($TiAl_3\square_4$), which is 0 0 0 4; 7b in the CaF_2 system (Table 6*b*; Hauck & Mika, 1998*a*). The f.c.c. lattices of the Zn or S atoms in ZnS or of Mg, Ag, As or vacancies □ in MgAg□As [Fig. 4A(*a*), deposited (or □NZnLi) can be combined in different ways to obtain the p.c. lattice [6 12 8; (1)] for Mg + Ag or □ + As combinations or the b.c.c. lattice for the Mg + Ag + As combination.

6. Conclusions

The present paper shows how the architecture of ordered body-centered, face-centered and primitive cubic structures/compounds can be analyzed using square planes. The crystal structures of A_xB_y compounds are characterized by the self-coordination numbers (s-CN) of the nearest (T_1), next-nearest (T_2) and third-nearest (T_3) neighbors and the composition y/x of the compound. The s-CN values are plotted in T_1, T_2 or α_1, α_2 structure maps where α_i are short-range order parameters, which are related to the T_i values as outlined in §1, step (vi). Structures found at the corners of these structure maps (Figs. 2 and 4–6) usually have high symmetry and the same T_1 T_2 T_3; y/x values for all A and for all B atoms. These structures can be decomposed into smaller structural units, *e.g.* v, v' and w', to construct structures that lie along the edges of the structure map and which can be characterized by sequences of structural units as *e.g.* $vw'v'_2w'v$ for the Ruddlesden–Popper phase Sr_2TiO_4 with w'_2 (SrO) and v_2 or v'_2 ($CaTiO_3$) as structural units (Hauck & Mika, 1997, 1998*b*; Parthé *et al.*, 1993).

We could identify approximately 55 structural units in b.c.c. and ~25 structural units in f.c.c. alloys. Most of the experimental structures are in six different families of crystal structures, which are named after the pioneers, *e.g.* the Ruddlesden–Popper phases. The structural units have identical square or in a few cases hexagonal planes which combine in different ways similar to a puzzle to give the different structures.

Most of the observed structures are at the right-hand border of the structure maps with low T_1. The interactions between A atoms vary continuously from attractive at low T_2 to repulsive at high T_2 values for different A_xB_y structures on the right-hand borders of the structure maps. The weakest interactions are found at the intersection with the line between $T_1 = T_2 = 0$ and T_1^{max}, T_2^{max} ($\alpha_1 = \alpha_2$).

Most structures with a single set of $T_i(A)$ values in Tables 2(*a*) and 4(*a*), and some structures in Table 6(*a*) are closely related, because they have identical space groups and Pearson symbols, but different distortions (§4). Structures with identical T_1 values can belong to the same type of homogeneous sphere packing of A atoms (Koch & Fischer, 1992). The

density $\rho_0 = 0.74$ of the f.c.c. Cu structure (type 2) for example is reduced to $\rho/\rho_0 = x/(x + y)$ in A_xB_y with vacant B positions. For structures on the left-hand borders of the structure maps containing alternating layers of A and B atoms, the packings of A atoms are not stable if the B atoms are removed. The group–subgroup relations (Bärnighausen, 1980; Müller, 1997), which can be arranged for the b.c.c., f.c.c. and p.c. systems (Tables 2–6 and 1A–3A, deposited), allow few space groups. In some structures with different space groups such as 4 2 2; 2a (Table 2*a*), 2 2 12; 2a (Table 4*a*) and 2 2 4; 2a (Table 6*a*) the projections of the crystal structure in the [111] direction are identical, but different in other directions. The Pearson symbol and sometimes also the space group will change in NaCl, ZnS or CaF_2 derivative structures, if all atom positions are included, or on vacancy formation. In some cases the structures of A_xB_y compounds can only be compared with the ordering of *e.g.* anions in NaCl or CaF_2 derivative structures as *e.g.* $\square Nb_3\square O_3$ or $Pr_7\square_2O_{12}$, if the location of the cations relative to the vacancies □ is added as additional information.

The position of a compound A_xB_y in the structure map can be different, as is outlined for the layered [001] and [111] structural series in Figs. 4–6. The formation of layered (001) (Schubert family) and (111) (Zalkin & Ramsey family) compounds with different compositions of the structural units in the b.c.c. system seems to be the consequence of the fact that most other series of structural units are not at the right-hand border of the structure map, as shown in Figs. 4A(*a*)–(*d*) (deposited) and 4. In the 0 6 12; 1 CsCl structure with an alternation of Cs and Cl atoms in the [001] or [111] direction, the Cs atoms are as far apart as possible with no nearest neighbor. A similar situation occurs in the 0 12 0; 1 ZnS structure of the p.c. lattice (Fig. 6), but not for the 4 6 8; 1 CuAu structure in the f.c.c. lattice with $T_1 = 4$ nearest Cu neighbors of Cu atoms (Fig. 5). Attractive interactions between A = Na, Cu, □ (or B = Tl, Pt, S) atoms are suggested for 4 0 12; 1 NaTl (Fig. 4) with the s-CN of 4 nearest and 0 next-nearest neighbors, the homometric 6 0 12; 1a,b CuPt a,b structures in the f.c.c. system (Fig. 5) and

Table 6

(*a*) s-CN values of theoretical primitive cubic alloys A_xB_y with single $T_i(A)$ and $T_i(B)$ values (M^i = 2, §2), $T_i(A)$ values of square planes perpendicular to the direction of highest symmetry, space group SG (*A* and *B* atoms) and Pearson symbol (PS), No. of reduced cell (Table 3A, deposited) and positions of atoms A_2–A_8.

$T_i(A)$; *y*/*x* p.c.	$T_i(A)$; *y*/*x* Square	SG	PS	No.	A_2 A_6	A_3 A_7	A_4 A_8	A_5
6 12 8; (1)	4 4 4; (1)	221	*cP*1	1				
5 8 4; 1	4 4 4; (1)	123	*tP*4	8	0 0 1			
(4 6 4; 1a)†	2 2 0; 1a	51	*oP*4	9	0 0 1			
(4 6 4; 1b)†	2 2 0; 1b	123	*tP*8	45	0 $\bar{1}$ 1	0 0 1	0 1 2	
(4 5 2; 1)†	2 1 2; 1	10	*mP*8	46	0 $\bar{1}$ 2	0 0 1	0 0 2	
4 4 0; 1	4 4 4; (1)	123	*tP*2	2				
(3 6 4; 1a)	6 6 6; (1)‡	166	*hR*12	12	1 0 0			
(3 6 4; 1b)	2 2 0; 1a	63	*oC*16	54	1 $\bar{1}$ $\bar{1}$	1 0 0	1 0 1	
(3 6 4; 1c)	2 2 0; 1b	225	*cF*64	77	0 1 1	1 0 1	1 1 0	1 1 1
					1 2 2	2 1 2	2 2 1	
(3 6 4; 1d)	2 2 0; 1b	160	*hR*48	77	0 1 1	1 0 1	1 1 0	1 1 1
					1 2 2	2 1 2	2 2 3	
(3 6 4; 1e)	2 2 0; 1b	141	*tI*32	77	0 1 1	1 0 1	1 1 0	1 1 1
					1 2 2	2 2 3	2 3 2	
(3 5 4; 1a)	2 1 2; 1	2	*aP*8	58	1 1 0	1 2 $\bar{1}$	1 2 0	
(3 5 4; 1b)	2 1 2; 1	5	*mC*32	76	0 $\bar{1}$ 1	0 $\bar{1}$ 2	0 0 1	1 $\bar{1}$ 1
					1 $\bar{1}$ 2	1 0 1	1 1 1	
(3 5 4; 1c)	2 1 2; 1	2	*aP*16	76	0 $\bar{1}$ 2	0 0 2	0 1 2	1 $\bar{1}$ 1
					1 $\bar{1}$ 2	1 0 1	1 1 1	
(3 5 4; 1d)	2 1 2; 1	43	*oF*64	76	0 $\bar{1}$ 1	0 $\bar{1}$ 2	0 1 2	1 $\bar{1}$ 1
					1 $\bar{1}$ 2	1 0 1	1 1 1	
(3 5 4; 1e)	2 1 2; 1	15	*mC*32	76	0 $\bar{1}$ 2	0 0 1	0 0 2	1 $\bar{1}$ 1
					1 $\bar{1}$ 2	1 0 1	1 1 1	
(3 5 4; 1f)	2 1 2; 1	12	*mC*32	76	0 $\bar{2}$ 1	0 0 2	0 1 2	1 $\bar{1}$ 1
					1 $\bar{1}$ 2	1 0 1	1 1 1	
3 4 4; 1a	3 2 2; 1	65	*oC*8	11	0 0 1			
3 4 4; 1b	2 0 4; 1	141	*tI*16	61	0 0 1	0 1 0	1 0 1	
(2 6 4; 1a)†	2 2 0; 1a	63	*oC*8	15	0 1 $\bar{1}$			
(2 6 4; 1b)†	2 2 0; 1b	139	*tI*16	62	1 0 1	1 1 0	2 1 1	
(2 5 6; 1)†	2 1 2; 1	12	*mC*16	57	0 1 $\bar{2}$	0 1 $\bar{1}$	1 0 $\bar{1}$	
2 4 8; 1	0 4 4; 1	123	*tP*2	3				
1 8 4; 1	0 4 4; 1	123	*tP*4	14	0 0 $\bar{1}$			
0 12 0; 1	0 4 4; 1	225	*cF*8	4				
(2 4 4; 1.3a)†	2 2 2; 1.3‡	146	*hR*21	40	0 1 0	1 1 0		
(2 4 4; 1.3b)†	2 2 2; 1.3‡	2	*aP*7	40	1 1 $\bar{1}$	1 1 0		
3 3 2; 1.5;	1 1 1; 1.5	10	*mP*5	19	0 0 1			
4 4 0; 2	2 0 2; 2	123	*tP*3	5				
2 2 4; 2a	0 2 0; 2	51	*oP*3	6				
2 2 4; 2b	0 6 0; 2‡	151	*hP*9	75	0 1 0	1 1 0		
2 2 2; 2	0 6 0; 2‡	2	*aP*9	74	1 1 $\bar{2}$	1 2 $\bar{2}$		
0 6 2; 2	6 6 6; (1)‡	164	*hP*3	7				
(1 2 3; 2.5)†	1 1 1; 2.5‡	2	*aP*7	40	0 1 0			
0 0 8; 3	0 0 4; 3	229	*cI*8	16				
2 0 0; 4	0 0 0 4; 4	83	*tP*5	19				
0 0 2; 6	0 0 0 6; 6	148	*hR*21	40				

† On the borders of the $T_1T_2T_3$;*y*/*x* polyhedron. ‡ Hexagonal planar.

(*b*) Different series of structures and $T_i(\square)$ values of $M_x\square_yO_z$ or CaF_2 derivative structures with a sequence of layers such as $A = \square$, B = O in Pb□O structure, space group SG and Pearson symbol PS for all atoms without vacancy position □ (Fig. 4A, deposited).

$M_x\square_yO_z$		SG	PS	$T_i(\square)$
CaF_2		225	*cF*12	6 12 8; (1)
EuOF		166	*hR*9	6 12 8; (1)
γ-LaOF, ZrH_2, $SiPt_2$		123	*tP*12	6 12 8; (1)
Layered (001) structures				
Pb□O	*AB*	129	*tP*4	4 4 0; 1
$M_3\square_2O_4$	AB_2	139	*tI*14	4 4 0; 2
$M_2\square O_3$	AB_3	129	*tP*10	4 4 0; 3
M□O	A_2B_2	123	*tP*8	5 8 4; 1
$M_3\square_2O_4$	$ABAB_3$	129	*tP*14	4 4 0; 2
M□O	ABA_2B_2	99	*tP*12	4.7 6.7 2.7; 1

Table 6 (continued)

$M_x\square_y O_z$		SG	PS	$T_i(\square)$
Layered (111) structures				
$M\square O$	AB	160	$hR6$	4 8 4; 1
$M_3\square_2O_4$	AB_2	164	$hP7$	0 6 2; 2
$M_2\square O_3$	AB_3	160	$hR15$	0 8 0; 3
$M\square O$	A_2B_2	166	$hR12$	3 6 4; 1a
$M_3\square_2O_4$	$ABAB_3$	156	$hP7$	3 6 3; 2
$M\square O$	ABA_2B_2	156	$hP6$	2 8 3.3; 1
Layered (110) structures with different composition $A = MO_2$, $A' = M_3O_6$, $A'' = M_4O_8$, $B = M\square_2$, $C = M\square O$, $D = M_3\square O_5$, $E = M_4\square O_7$, $F = M_7\square_2O_{12}$, $G = M_{11}\square_2O_{20}$ (Thornber & Bevan, 1970)				
$Pt\square S$	AB	131	$tP4$	2 4 8; 1
$M_3\square_2O_4$	AB_2	65	$oC6$	2 2 4; 2a
$M_2\square O_3$	AB_3	47	$oP4$	2 2 4; 3
$M\square O$	A_2B_2	51	$oP4$	4 6 4; 1a
$M_3\square_2O_4$	$ABAB_3$	47	$oP6$	2 3 6; 2
$M\square O$	ABA_2B_2	25	$oP6$	3.3 5.3 5.3; 1
$Cu_2\square_3O$	BC	224/201	$cP6$	0 0 8; 3
$Pr_7\square_2O_{12}$	F	148	$hR57$	0 0 2; 6
$Pr_9\square_2O_{16}$	$A'D_2$	2	$aP25$	0 0 1; 8
$(Ce_{21}\square_4O_{38})$	$A'DA'D_2A'D$			
$(Ce_{19}\square_4O_{34})$	$A'D(A'D_2)_3A'D(A'D_2)_2$ or $A''E_5A''E_6A''E_5$			
$Pr_{10}\square_2O_{18}$	$A''E_4$	11	$mP112$	0 0 1; 9
$Pr_{12}\square_2O_{22}$	$A''E_2$	11	$mP68$	0 0 0 0 3; 11
$Tb_{11}\square_2O_{20}$	G	2	$aP31$	0 0 0 0 4; 10

(*c*) ZnS family and other $A_xB_yC_z$ structures with $T_i(A/B)$

$A_xB_yC_z$	SG	PS	$T_i(A/B)$
ZnS family			
$Zn\square S$	216	$cF8$	0 12 0; 1
$MgAg\square As$	216	$cF12$	0 12 0; 1
$\square NZnLi$	216	$cF12$	0 12 0; 1
$\square CdIn_2Se_4$	111	$tP7$	0 0 0; 7a
$SbCu_3S_4$	121	$tI16$	0 0 0; 7b
$CuFeS_2$	122	$tI16$	0 4 0; 3b
α-$Zn\square_3Cl_2$	122	$tI12$	0 4 0; 3b
(Ga,As)(Al,As)	115	$tP4$	0 4 0; 3c
$In(Ga,Al)P_2$	160	$hR4$	0 6 0; 3
$GeCu_2Se_3$	44	$oI12$	0 2 0; 5a
β-$\square Ga_2Se_3$	9	$mC20$	0 2 0; 5e
$NiSi_2Cu_4S_7$	5	$mC28$	0 1 0; 6
$(Ga, As)_2(Al, As)_2$	115	$tP8$	0 8 0; 3
$(Ga,As)(Al,As)_2$	119	$tI12$	0 4 0; 5
Other compounds			
$Si\square_3S_2$	72	$oI12$	2 0 0; 3
Li_3AlN_2	206	$cI96$	0 3 2; 3
$(Fe, Mn)_2\square O_3$	206	$cI80$	0 3 2; 3
$Hg\square_3I_2$	137	$tP12$	0 4 0; 3a
$Sn\square_7I_4$	205	$cP40$	0 0 1; 7
Li_7VN_4	218	$cP96$	0 0 0 1.5; 7
β-$Li_5Al\square_2O_4$	59	$oP20$	0 0 0 2; 7/ 0 2 4; 3
β-$Li_5Ga\square_2O_4$	21	$oC40$	0 0 0 2; 7/ 0 0 8 6; 3
$Li_5Tl\square_2O_4$	137	$tP80$	0 0 0 4; 7/ 0 5 0; 3
$Na_6Pb\square O_4$	217	$cI88$	0 3 0 0; 7 (Pb,□)

the 2 4 8; 1 Pt□S structure (Fig. 4A, deposited) in the p.c. system.

Two other principles of structure formation besides the combinations of structural units were observed in the present investigation: A stepwise filling of atom positions in homologous structures such as $AuCu_3$ (0 6 0; 3), AuCu (4 6 8; 1), Cu_3Au (8 6 16; 0.3), Cu [12 6 24; (1)] with $T_1 = 0, 4, 8, 12$, $T_2 = 6$ and $T_3 = 0, 8, 16, 24$ (Table 5) and identical α_i values. In quasi-homologous series of structures (different α_i values) the different combinations of the 0 0 12; 3 structure of Sn, Mg, Li and Pd atoms in SnMgLiPd give rise to the $AgSbLi_2$, $AlMnCu_2$ and NaTl structures [Table 2*b*, Fig. 2A(*a*) deposited] with different α_i values.

A similar situation occurs for magnetic structures (Oleś *et al.*, 1976) with an ordering of two spin directions $\oplus$ and $\ominus$ at Mn atoms in MnS_2 or $MnTe_2$, where the ordering for example follows the $UPb\square_4$ type (4 4 16; 1) or the $CuAu\square_4$ type (4 6 8; 1) structures and $MnSe_2$ has a structure with intermediate T_i values 4 4.7 13.3; 1. The four spin directions of the Dy atoms in $DyAlO_3$ are combined in the same way as the four atoms in a quaternary alloy such as SnMgLiPd (Hauck & Mika, 2000*c*). The ordering of magnetic moments in the same structures as the ordering of metal atoms in alloys supports a different view of sphere packing, which has been discussed for many centuries (Brunner, 1971), *e.g.* the statement of Boscovich (1758): 'Atoms are centres of interactions whose diameters are negligible or of minor interest as compared to their separations'.

The principle of filling sites in a given structure is similar to the way we obtained the different structures. We determined the reduced unit cells with single occupation (Tables 1A–3A deposited) and obtained all structures of the structure maps by occupation of other positions. The observed structures of the homologous and quasi-homologous series are a small selection, where α_i values do not change or change only along the boundary of the structure map, respectively. These structures with maximum attractive or repulsive interactions between A (or B) atoms are stabilized by enthalpy.

We acknowledge the support of K. Bickmann and D. Henkel, IFF with the preparation of the figures and the text.

References

Allen, S. M. & Cahn, J. W. (1972). *Acta Metall.* **20**, 423–433.

Bärnighausen, H. (1980). *MATCH, Commun. Math. Chem.* **9**, 139–175.

Brauer, G. (1939). *Z. Anorg. Allg. Chem.* **242**, 1–22.

Brunner, G. O. (1971). *Acta Cryst.* A**27**, 388–390.

Burdett, J. K. (1995). *Chemical Bonding in Solids.* Oxford University Press.

Chattopadhyay, K., Lele, S., Thangaraj, N. & Ranganathan, S. (1987). *Acta Metall.* **35**, 727–733.

Donohue, J. (1974). *The Structures of the Elements.* New York: John Wiley.

Ducastelle, F. (1991). *Cohesion and Structure*, Vol. 3, *Order and Phase Stability in Alloys*, edited by F. R. de Boer and D. G. Pettifor. Amsterdam: North-Holland.

Finel, A. & Ducastelle, F. (1984). *Mater. Res. Soc. Symp. Proc.* **21**, 293–298.

Forsyth, J. B. & Gran, G. (1962). *Acta Cryst.* **15**, 100–104.

Galasso, F. S. (1970). *Structure and Properties of Inorganic Solids.* Oxford: Pergamon Press.

Hauck, J. (1980). *Acta Cryst.* A**36**, 228–237.

Hauck, J., Henkel, D., Klein, M. & Mika, K. (1999). *J. Solid State Chem.* **145**, 150–158.

Hauck, J., Henkel, D. & Mika, K. (1988*a*). *Physica C*, **153–155**, 1173–1174.

Hauck, J., Henkel, D. & Mika, K. (1988*b*). *Z. Phys. B*, **71**, 187–192.

Hauck, J., Henkel, D. & Mika, K. (1988*c*). *Z. Kristallogr.* **182**, 124–127.

Hauck, J., Henkel, D. & Mika, K. (1988*d*). *Z. Kristallogr.* **182**, 297–306.

Hauck, J., Henkel, D. & Mika, K. (1989). *Int. J. Mod. Phys. B*, **3**, 1425–1433.

Hauck, J. & Mika, K. (1993). *Int. J. Mod. Phys. B*, **7**, 3423–3433.

Hauck, J. & Mika, K. (1994). *Intermetallic Compounds*, Vol. 1, *Principles*, edited by J. H. Westbrook and R. L. Fleischer, pp. 277–307. London: Wiley.

Hauck, J. & Mika, K. (1997). *Studies of High Temperature Superconductors*, Vol. 25, edited by A. V. Narlikar, pp. 1–74. Commack New York: Nova Science.

Hauck, J. & Mika, K. (1998*a*). *J. Solid State Chem.* **138**, 334–341.

Hauck, J. & Mika, K. (1998*b*). *Supercond. Sci. Technol.* **11**, 614–630.

Hauck, J. & Mika, K. (2000*a*). *Solid State Ion.* **127**, 1–21.

Hauck, J. & Mika, K. (2000*b*). *Surface Rev. Lett.* In the press.

Hauck, J. & Mika, K. (2000*c*). *J. Magn. Magn. Mater.* **212**, 389–400.

Ho, S.-M. & Douglas, B. E. (1968). *J. Chem. Educ.* **45**, 474–476.

Hoppe, R. & Panek, P. (1971). *Z. Anorg. Allg. Chem.* **381**, 129–139.

Hyde, B. G. & Andersson, S. (1989). *Inorganic Crystal Structures.* New York: Wiley.

Johansson, C. H. & Linde, J. O. (1936). *Ann. Physik*, **25**, 1–48.

Juza, R., Gieren, W. & Haug, J. (1959). *Z. Anorg. Allg. Chem.* **300**, 61–71.

Kanamori, J. & Kakehashi, Y. (1977). *J. Phys.* Colloque 7, 274–279.

Ketelaar, J. A. A. (1935). *Z. Kristallogr. A*, **90**, 237–255.

Ketelaar, J. A. A., MacGillavry, C. H. & Renes, P. A. (1947). *Rec. Trav. Chim. Pays-Bas*, **66**, 501–512.

Koch, E. & Fischer, W. (1992). *International Tables for Crystallography*, edited by A. J. C. Wilson, Vol. C, pp. 654–659. Dordrecht: Kluwer Academic Publishers.

Kripyakevich, P. I. & Grin, Yu. N. (1979). *Sov. Phys. Crystallogr.* **24**, 41–44.

Křivý, I. & Gruber, B. (1976). *Acta Cryst.* A**32**, 297–298.

MacLaren, J. M., Pendry, J. B., Rous, P. J., Saldin, D. K., Somorjai, G. A., Van Hove, M. A. & Vvedensky, D. D. (1987). *Surface Crystallographic Information Service: A Handbook of Surface Structures.* Dordrecht: Reidel.

Mika, K., Hauck, J. & Funk-Kath, U. (1994). *J. Appl. Cryst.* **27**, 1052–1055.

Mika, K., Henkel, D. & Hauck, J. (1989). *Z. Kristallogr.* **186**, 202–204.

Müller, U. (1991). *Anorganische Strukturchemie.* Stuttgart: Teubner.

Müller, U. (1997). *Predictability of Crystal Structures of Inorganic Solids*, edited by H. Burzlaff, pp. 74–81. Hünfeld 27.10–30.10. To be published.

Oleś, A., Kajzar, F., Kucab, M. & Sikora, W. (1976). *Magnetic Structures by Neutron Diffraction.* Warszawa: Państwowe Wydawnictwo Nakowe.

Panek, P. & Hoppe, R. (1973). *Z. Anorg. Allg. Chem.* **400**, 208–218.

Pani, M. & Fornasini, M. L. (1990). *Z. Kristallogr.* **190**, 127–133.

Parthé, E., Gelato, L., Chabot, B., Penzo, M., Cenzual, K. & Gladyshevskii, R. (1993). *TYPIX: Standardized Data and Crystal Chemical Characterization of Inorganic Structure Types*, Vol. 1, *Gmelin Handbook of Inorganic and Organometallic Chemistry.* Berlin: Springer.

Pauling, L. (1929). *J. Am. Chem. Soc.* **51**, 1010–1026.

Pauling, L. (1960). *The Nature of the Chemical Bond.* Ithaca, New York: Cornell University Press.

Pearson, W. B. (1972). *The Crystal Chemistry and Physics of Metals and Alloys.* New York: Wiley.

Sanchez, J. M. & de Fontaine, D. (1981). *Structure and Bonding in Crystals*, Vol. II, edited by M. O'Keeffe and A. Navrotsky, pp. 117–132. New York: Academic Press.

Sato, H. & Toth, R. S. (1965). *Metallur. Soc. Conf.* **29**, 295–419.

Schubert, K. (1964). *Kristallstrukturen zweikomponentiger Phasen.* Berlin: Springer.

Schubert, K., Anantharaman, T. R., Ata, H. O. K., Meissner, H. G., Pötzschke, M., Rossteutscher, W. & Stolz, E. (1960). *Die Naturwiss.* **47**, 512.

Schubert, K., Meissner, H. G. & Rossteutscher, W. (1964). *Die Naturwiss.* **51**, 507.

Schweda, E., Bevan, D. J. M. & Eyring, L. (1991). *J. Solid State Chem.* **90**, 109–125.

Sohncke, L. (1879). *Entwicklung einer Theorie der Kristallstruktur*, p. 23. Leipzig: B. G. Teubner.

Stewner, F. & Hoppe, R. (1971*a*). *Z. Anorg. Allg. Chem.* **381**, 140–148.

Stewner, F. & Hoppe, R. (1971*b*). *Z. Anorg. Allg. Chem.* **381**, 149–160.

Teuho, J., Mäki, J. & Hiraga, K. (1987). *Acta Metall.* **35**, 721–725.

Thornber, M. R. & Bevan, D. J. M. (1970). *J. Solid State Chem.* **1**, 536–544.

Villars, P. & Calvert, L. D. (1986). *Pearson's Handbook of Crystallographic Data for Intermetallic Phases*, Vols. 1–3. Metals Park, OH: American Society for Metals.

Wiener, C. (1863). *Die Grundzüge der Weltordnung. I: Atomlehre*, p. 82. Leipzig und Heidelberg: Winter.

Wyckoff, R. W. G. (1982). *Crystal Structures*, Vols. 1–3. Krieger: Malabar, FL.

Zalkin, A. & Ramsey, W. J. (1956). *J. Phys. Chem.* **60**, 234–236.

Zalkin, A., Ramsey, W. J. & Templeton, D. H. (1956). *J. Phys. Chem.* **60**, 1275–1277.

Zhang, J., Von Dreele, R. B. & Eyring, L. (1993). *J. Solid State Chem.* **104**, 21–32.

Zhang, J., Von Dreele, R. B. & Eyring, L. (1995*a*). *J. Solid State Chem.* **118**, 133–140.

Zhang, J., Von Dreele, R. B. & Eyring, L. (1995*b*). *J. Solid State Chem.* **118**, 141–147.

Zhang, J., Von Dreele, R. B. & Eyring, L. (1996). *J. Solid State Chem.* **122**, 53–58.